Analysis of Free-vibration and Linear Elastic Fracture Mechanics Problems Using Polygonal Finite Elements with Schwarz-Christoffel Conformal Mapping.

A Project Report

Submitted in partial fulfilment of the

requirements for the Degree of

Master of Engineering

in

Aerospace Engineering

by

K Tulaseeram

Department of Aerospace Engineering

Indian Institute of Science

BANGALORE – 560 012

July 2009

TO

My Parents

Savithree Kondamchetty

Nagaraja Kondamchetty

Acknowledgements

I started my project work with limited background knowledge and encountered numerous problems during my studies. **Prof. D. Roy Mahapatra** carried me through all the difficulties since my first day in the project. My work wouldnt have been possible without his endless support. More importantly, as a guide, he always inspired me with enlightening ideas and always gave me generous help and encouragement. As a teacher, he often explained project to me in simple and precise language. My most sincere thanks go to him first.

I would like to express my thanks to the **Prof. B N Raghunandan**, Ex-Chairman, Department of Aerospace Engineering, **Prof. M.S. Bhatt**, Chairman, Department of Aerospace Engineering for providing me an excellent work environment and computing facilities in the department. My thanks also go to all faculty members and staff of the Aerospace Department.

I would like to thank my lab mates Kannan, Sundeep, Indrajith, Vadiraj, Ahish, Abhishek, Nibir, and Vivek who have been a constant source of support and inspiration for me. I wish to thank my fellow students and friends,Krishna Kishore, Narendar, Sushma, Sudeesh, Varaprasad, Vivekanad, and Sreehari who helped me in solving research problems and gave me a lot of laugh in my student life.

I would also like to thank Sundararajan Natarajan, Phd scholar, University of Glasgow, Glasgow, U.K, for his valuable support in my project work.

I would like to dedicate this work to my family, which has been supporting me in achieving all my aspirations and ventures.

K Tulaseeram,

Structures Laboratory,

Department of Aerospace Engg.,

Indian Institute of Science, Bangalore.

Abstract

The finite element method is the ubiquitous choice to solve boundary-value problems in solid mechanics. In two-dimensions, the constant strain triangular element and the quadrilateral element are widely used in research as well as in industrial practice. Quadrilateral and triangular elements with higher order interpolants are also used to improve accuracy. Polygonal finite elements provide greater flexibility in mesh generation than quadrilateral or triangular elements and are better-suited for applications in solid mechanics which involve a significant change in the topology of the material domain. Polygonal elements can be used in the analysis of polycrystalline material without further discretization which is otherwise required in standard FEM. The development of finite elements on irregular polygons has not been explored to any significant depth so far. In this work, a new integration technique is used to integrate the weak form of the governing partial differential equation over the polygon. Solving linear elastic fracture mechanics (LEFM) problem using standard finite element method requires fine mesh, and geometry of the mesh should conform with the crack geometry in the domain. For each crack, a separate refinement to the crack is required to solve the LEFM problem with remeshing for a new crack dimension. Mesh refinement and meshing can be avoided by using Extended Finite Element Method, in which a back ground mesh without crack can be used to solve the LEFM problem. In XFEM using Gauss quadrature method, elements can not have more than four edges and convexity of the elements need to be ensured to have positive jacobian. In this work an XFEM using polygonal finite element method is proposed using the new integration scheme on polygon. This method avoids subdivision of elements for integration having discontinuities, which is otherwise required in XFEM using standard

finite element method. The overall approach is validated using a successful convergence study of a elasto-static, free vibration and mode-I crack in a thick beam bending problem.

Keywords

Polygonal Finite Element, Shawarz-Christoffel conformal Mapping, Free vibration, Extended Finite Element Method, Wachspress shape function, Numerical integration, J-integral, Stress intensity factor computation.

Contents

List of Tables

List of Figures

Chapter 1

Introduction

1.1 Polygonal finite element method: An Introduction

The Finite Element Method (FEM) is a mathematical and numerical method to solve physical problems governed by partial differential equations on a finite domain. Usually the problems addressed using FEM are too complicated to be solved satisfactorily by analytical methods. The problem may concern stress analysis, heat conduction, structural vibration, fluid flow or any of several other areas. The finite element procedure produces many simultaneous algebraic equations, which are generated and solved on a computer. Results are not always exact. However, errors are decreased by processing more equations until the results become accurate enough to apply in the corresponding engineering problems at reasonable cost. The finite element method originated as a method of stress analysis. Today finite elements are also used to analyze problems of heat transfer, fluid flow, lubrication, electric and magnetic fields, and many other problems. The power of the finite element method resides principally in its versatility. The method can be applied to various physical problems. The body analyzed can have arbitrary shape, loads, and support conditions. The mesh can mix elements of different types, shapes, and physical properties. This great versatility is contained within a single

computer. User prepared input data controls the selection of problem type, geometry, boundary conditions, element selection and so on.

In the beginning 1906, researchers suggested a "Lattice analogy" for stress analysis. The continuum was replaced by a regular pattern of elastic bars. Properties of the bars were chosen in a way that caused displacements of the joints to approximate displacement of points in the continuum. The method sought to capitalize on well-known methods of structural analysis. Courant appears to have been the first to propose the finite element method as we know it today. In a 1941 mathematics lecture, published in 1943, he used the principle of stationary potential energy and piecewise polynomial interpolation over triangular subregions to study the Saint-Venant torsion problem [1]. FEM now becomes very powerful technique in stress analysis, structural vibration, heat flow, fluid flow and several other areas. FEM is an approximate method, and accuracy of the solution can be increased by mesh refinement. The extent of accuracy requirement depends upon the nature and application of engineering problem. Very fine mesh should be used to have better accuracy of the solution. Stress analysis and structural dynamics for simple geometry can be solved using analytical method and it is difficult to solve for the complex geometries using analytical method. For such problems FEM can be used to solve the structural dynamics and stress analysis problems.

Introduction and fast development of the finite element method drastically changed the extent of application of Linear Elastic Fracture Mechanics (LEFM). FEM virtually had no limitation in solving complex geometries and loading conditions, and soon it was extended to nonlinear materials and large deformations problems [2]. As a result, LEFM solutions could now rely on powerful analytical tool in order to determine its fundamental concepts and governing criteria such as crack energy release rate and the stress intensity factor for any complex problem. General LEFM stability criteria could then be used to asses the stability or propagation of an existing crack. Application of FEM into linear elastic fracture mechanics has now expanded to almost all types of crack problems. But handling discontinuity is a major problem to analyse a continua having discontinuity. This problem can be minimized by meshing the domain in such a way that the crack

geometry should conform the mesh geometry. Moreover mesh refinement is a difficult task and method become very cumbersome for crack propagation problem. Parametric studies and experimental observations have been resulted in the introduction of new design codes for containing a stable crack. However, the essence of analysis remained almost same: Basics concepts of LEFM combined with classical continuum based FEM techniques through smeared or discrete crack models. After a few decades, a major break through seemed to be evolving in the fundamental idea of partition of unity in the form of the extended Finite Element Method (XFEM).

1.1.1 Various types of finite element methods

1. **hp-FEM**

   The hp-FEM [5] combines adaptively elements with variable size h and polynomial degree p in order to achieve exceptionally fast, exponential convergence rates. The hp-FEM is a general version of the FEM, a numerical method for solving partial differential equations based on piecewise-polynomial approximations that employs elements of variable size (h) and polynomial degree (p). The origins of hp-FEM date back to the pioneering work of Ivo Babuska et al [6] who discovered that the FEM converges exponentially fast when the mesh is refined using a suitable combination of h-refinements (dividing elements into smaller ones) and p-refinements (increasing their polynomial degree). The exponential convergence makes the method a very attractive choice compared to most other finite element methods which only converge with an algebraic rate. Smooth functions can be approximated much more efficiently using large high-order elements than small piecewise-linear ones. In standard FEM one only works with shape functions associated with grid vertices (the so-called vertex functions). In contrast to that, in the hp-FEM one moreover edge functions (associated with element edges), face functions (corresponding to element faces - 3D only), and bubble functions (higher-order polynomials which vanish on element boundaries).

2. **Generalized finite element method**

   The Generalized Finite Element Method [7] (FEM) uses local spaces consisting of functions, not necessarily polynomials, that reflect the available information on the unknown solution and thus ensure good local approximation. Then a partition of unity is used to bond these spaces together to form the approximating subspace. The effectiveness of GFEM has been shown when applied to problems with domains having complicated boundaries, problems with micro-scales, and problems with boundary layers.

3. **Extended finite element method (XFEM)**

   The extended finite element method (XFEM) [13], also known as generalized finite element method (GFEM) or partition of unity method (PUM) is a numerical technique that extends the classical finite element method (FEM) approach by extending the solution space for solutions to differential equations with discontinuous functions.The extended finite element method (XFEM) is used to alleviate the above shortcomings of the finite element method and has been used to model the propagation of various discontinuities: strong (cracks) and weak (material interfaces). The principle idea behind XFEM is to retain most advantages of mesh-free methods while alleviating their negative sides. Enriched finite element methods extend, or enrich, the approximation space so that it is able to naturally reproduce the challenging feature associated with the problem of interest: the discontinuity, singularity, boundary layer, etc. It was shown that for some problems, such an embedding of the problem's feature into the approximation space can significantly improve convergence rates and accuracy. Moreover, treating problems with discontinuities with eXtended Finite Element Methods suppresses the need to mesh refinement and the need of remeshing the discontinuity surfaces, thus reducing the computational costs and projection errors associated with conventional finite element methods, at the cost of restricting the discontinuities to mesh edges.

4. **Spectral method**

   Spectral methods [4] are a class of techniques used in applied mathematics and scientific computing to numerically solve certain partial differential equations (PDEs), often involving the use of the Fast Fourier Transform. Where applicable, spectral methods have excellent error properties, with the so called "exponential convergence" being the fastest possible.

   PDEs describe a wide array of physical processes such as heat conduction, fluid flow, and sound propagation. In many such equations, there are underlying "basic waves" that can be used to give efficient algorithms for computing solutions to these PDEs. In a typical case, spectral methods take advantage of this fact by writing the solution as its Fourier series, substituting this series into the PDE to get a system of ordinary differential equations (ODEs) in the time-dependent coefficients of the trigonometric terms in the series (written in complex exponential form), and using a time-stepping method to solve those ODEs.

   The spectral method and the finite element method are closely related and built on the same ideas; the main difference between them is that the spectral method approximates the solution as linear combination of continuous functions that are generally nonzero over the domain of solution (usually sinusoids or Chebyshev polynomials), while the finite element method approximates the solution as a linear combination of piecewise functions that are nonzero on small subdomains. Because of this, the spectral method takes on a global approach while the finite element method is a local approach. This is part of why the spectral method works best when the solution is smooth. In fact there are no known three-dimensional single domain spectral shock capturing results. Modeling of elastic wave propagation in plates given in [38], is based on the partition of unity approach, in which the approximate spectral properties of the infinite dimensional system are embedded within the space of a conventional finite element method through a consistent technique of waveform enrichment. The technique is general, such that it can be applied to the Lagrangian family of finite elements with specific waveform enrichment schemes,

depending on the dominant modes of wave propagation in the physical system.

In the finite element community, a method where the degree of the elements is very high or increases as the grid parameter h decreases to zero is sometimes called a spectral element method.

The implementation of the spectral method is normally accomplished either with collocation or a Galerkin approach.

5. **Meshfree methods**

   Meshfree methods have been recently reviewed and classified in [3]. Meshfree methods are a particular class of numerical simulation algorithms for the simulation of physical phenomena. Traditional simulation algorithms relied on a grid or a mesh, meshfree methods in contrast use the geometry of the simulated object directly for calculations. Meshfree methods exist for fluid dynamics as well as for solid mechanics. Some methods are able to handle both cases. Meshfree methods eliminate some or all of the traditional mesh-based view of the computational domain and rely on a particle (either Lagrangian or Eulerian) view of the field problem.

   A goal of meshfree methods is to facilitate the simulation of increasingly demanding problems that require the ability to treat large deformations, advanced materials, complex geometry, nonlinear material behavior, discontinuities and singularities. For example the melting of a solid or the freezing process can be simulated using meshfree methods.

   Meshfree (or 'meshless' as this is also used) methods seem attractive as alternative to finite element method (FEM) for the general engineering community, which consider the process of generating finite element meshes as more difficult and expensive than the remainder of analysis process.

6. **Galerkin methods**

   In mathematics, in the area of numerical analysis, Galerkin methods are a class of methods for converting a continuous operator problem (such as a differential equation) to a discrete problem. In principle, it is the equivalent of applying the method

of variation to a function space, by converting the equation to a weak formulation. Typically one then applies some constraints on the functions space to characterize the space with a finite set of basis functions. Often when using a Galerkin method one also gives the name along with typical approximation methods used, such as Petrov-Galerkin method or Ritz-Galerkin method [8]. The approach is credited to the Russian mathematician Boris Galerkin.

Mapped elements, such as the well-known isoparametric elements play a vital role in the conventional Finite Element Method (FEM). In an effort to overcome the limitations of FEM, mesh free methods were introduced. Although there are many different types of meshfree methods, it seems consensual that they are in general superior to Finite Element methods for problems where large transformations are of interest and when high order continuity of the solution is required. However, it also seems clear from the literature that most meshfree methods, especially those relying on a weak form, are more computationally expensive than finite elements. Handling discontinuities in meshfree methods also seems more straightforward as in standard FEM because no meshing or remeshing of the evolving discontinuities is required.

Melenk and Babu has introduced the extended (generalized) Finite element method (XFEM) to bridge the gap between FEMs and meshfree methods. These methods share advantages with both the meshfree and standard FEMs. They rely on simple underlying polynomial shape functions (as in FEM) and are enriched by suitable functions (discontinuous or other) to capture known features of the solution. These partition of unity based Finite element methods, however, do not solve the problem associated with mesh distortion mentioned above. What is more, they still require the domain to be discretized (meshed) using a combination of triangles and quadrilaterals (in 2D), unless recourse is made to implicit boundary definition, which causes additional difficulties in imposing boundary conditions and ensuring an accurate definition of the boundary of the domain. In an effort to alleviate the meshing requirement and mesh-distortion sensitivity of the FEM, two recent avenues of investigation have spurred the interest of researchers:

1. Smoothed Finite element methods

   In this method there is no need for iso parametric mapping, and thus method yields accurate results even for extreamly distorted meshes. This idea was proposed by Liu [9] and developed for plates, shells, plate cracking and 3D continuum, 2D elasto-plasticity and plate vibration and shown to yield accurate results.

2. Polygonal Finite element methods.

   In a similar way to alleviate the constraints imposed on standard finite element method, polygonal elements have gained of research interest. Polygonal elements provide greater flexibility in meshing and better accuracy. Polygonal elements also called n - *gon* elements (n is the number of vertices in the polygon). n - *gon* elements can be used as a transition elements and polycrystalline material to represent microstructure of polycrystalline alloys. However, approximation functions on polygons are usually non-polynomial, which causes numerical integration difficulties.

In standard Finite Element method, integration points can be located by simple transformation of physical element to master element configuration. For n - gon element there is no such transformation is available. In most of the polygonal finite element methods *Gauß* integration is in exact, because the approximation space is non-polynomial. Similar kind of difficulties arise in enriched FEM, such as XFEM, where non-polynomial functions are used, or to integrate discontinuous functions over elements split by discontinuous functions over elements split by discontinuities. To integrate these non-polynomial functions with a sufficient level of precision, in practice, many *Gauß* points are used. Integration over the polygonal element has not reached to matured stage. Efficient and robust integration scheme to integrate the weak form of differential equations over n - gon element. So far there are two integration schemes are available to integrate over the n - gon element.

1. Numerical integration of weak form over the n - gon described by Sukumar and Tabarraei [10], in which irregular polygon is mapped to regular polygon and further

subdivided into triangles. And then *Gauß* quadrature rule is applied over the triangle to integrate the weak form. In this method there exist two level of mapping. Meshing of the domain should ensure the convexity of the element to avoid negative jacobian.

2. A new rule based on schawrz christoffel conformal mapping to integrate weak form over the$n$ - gon proposed by Sundararajan *et al* [11]. In this method physical element (n - gon element) is mapped onto a unit disk, preserving angle between the vertices, using Schwarz-Christoffel conformal mapping. And then, integration is carried over the unit disk [12] using various cubature rules. Here, only one level of mapping is required and since, positivity of jacobian is always guaranteed irrespective of convexity of the element, there is high flexibility in meshing.

1.1.2 Extended Finite Element Method

Modeling of fracture and failure remains one of the most challenging problems in mechanics. Finite element analysis using singular elements as well as enriched elements are reasonably effective in the analysis of stationery cracks. To model a crack using these methods, meshing should conform to the crack geometry and complexity further increases if the crack is irregular. To avoid these difficulties an extended Finite Element Method (XFEM) has been proposed by Belytschko and Dolbow [13]. In this method crack is modeled using a background mesh and elements in which crack exists are enriched. Elements used are of triangular or quadrilateral shapes. For domains having complex geometry very fine mesh is required near the stress concentration regions. Moreover, convexity of the element should be maintained to avoid negative jacobian. As a consequence cost of computation is high for such complex geometry. Polygonal finite elements are a generalization of triangular and quadrilateral finite element methods to meshes with n-sided elements ($n \geq 3$). Polygonal finite elements provide greater flexibility in meshing.

1.2 Problem and Motivation

Though standard Finite Element Method (FEM) is the ubiquitous choice to solve the boundary-value problems in solid mechanics, has following disadvantages

1. Static analysis and dynamic analysis of the structures for complex geometries require very fine mesh to model the geometry with matching wave length. Therefore more number of elements are required to have better approximate solution.

2. Convexity of the element should be ensured to avoid negative jacobian.

3. Mesh used in the FEM should have less distorted elements and to have better approximate solutions.

4. Quadrilateral elements or triangular elements do not provide greater flexibility in meshing the complex geometries.

5. Handling discontinuity like cracks is a difficult task in the standard FEM. This difficulty can be handled by using XFEM proposed by Belytschko and Dolbow [13] which uses a back ground mesh without crack to model the crack. But for complex geometries a fine mesh is required to have better approximate solution.

In this thesis work polygonal finite element method is developed as polygonal elements provide greater flexibility in meshing complex geometries. And mesh distortion sensitivity, positivity of the jacobian are studied in this work.

1.3 Scope of the Thesis

The present work involves the formulation of the polygonal finite element using Schawrz-Christoffel conformal mapping for static, free vibration and linear elastic fracture mechanics problems in structural mechanics. In Chapter 2 formulation about Schawrz-Christoffel conformal mapping, derivation of jacobian, cubature integration rule over the unit disk and construction of interpolation functions on the n-gon is given. In chapter 3

polygonal finite element formulation for static and free vibration of a cantilever beam, and the convergence of the method is studied. In chapter 4 formulation of Extended polygonal finite element method using schwarz-christoffel conformal mapping for linear elastic crack problems is given. Conclusion and future scope the work is given in chapter 5.

Chapter 2

Numerical Integration Of Weak Form on Polygon

The governing equilibrium equations for a 2D static elasticity problem defined in the domain Ω bounded by Γ and $\Gamma = \Gamma_u \cup \Gamma_t$, $\Gamma_u \cap \Gamma_t = \phi$

$$\nabla_s^{\mathrm{T}} \boldsymbol{\sigma} + \mathbf{b} = \mathbf{0} \quad \text{in } \Omega \tag{2.1}$$

Where $\mathbf{0}$ is a null vector, $\boldsymbol{\sigma}$is the stress tensor and b is the vector of external forces. The following are the prescribed boundary conditions

$$\mathbf{u} = \overline{\mathbf{u}} \ \textit{in} \ \Gamma_u \tag{2.2}$$

$$\mathbf{n}^T \boldsymbol{\sigma} = \bar{\mathbf{t}} \ \textit{on} \ \Gamma_t \tag{2.3}$$

where $\overline{\mathbf{u}} = (\overline{u}_x, \overline{u}_y)^T$ is the prescribed displacement vector on the essential boundary Γ_u;

$\mathbf{t} = (\bar{t}_x, \bar{t}_y)^T$ is the prescribed traction vector on the natural boundary Γ_t; $\mathbf{n}$ is the unit outward normal vector. The discrete equations for this problem are generated from the

Galekin weak form

$$\int_{\Omega} (\bigtriangledown_s \delta\mathbf{u})^T \mathbb{D} (\bigtriangledown_s \delta\mathbf{u}) d\Omega - \int_{\Gamma} (\delta\mathbf{u}^T)\mathbf{b} d\Omega - \int_{\Gamma} (\delta\mathbf{u})^T \bar{\mathbf{t}} d\Gamma = 0 \tag{2.4}$$

where $\mathbf{u}$ and $\delta\mathbf{u}$ are the test functions that belong to Sobolev space of functions and $\mathbb{D}$ is the constitutive matrix. The Finite element method uses the following trial and test functions:

$$\mathbf{u}^h(\mathbf{x}) = \sum_{i=1}^{NP} \mathbf{N}_i(\mathbf{X})\mathbf{d}_i, \quad \delta\mathbf{u}^h(\mathbf{x}) = \sum_{i=1}^{NP} \mathbf{N}_i(\mathbf{X})\delta\mathbf{d}_i \tag{2.5}$$

where NP is the total number of nodes in the mesh.

$$\mathbf{N}_i = \begin{bmatrix} N_i & 0 \\ 0 & N_i \end{bmatrix} \tag{2.6}$$

is the shape functions matrix of degree p associated with node i, $\mathbf{d}_i = [u_i, v_i]^T$ are the degrees of freedom associated with node i By substituting the approximations, $\mathbf{u}^h$ and $\delta\mathbf{u}^h$, into the weak form and invoking the arbitrariness of virtual nodal displacements, Eq.(2.5) yields the standard discretized algebraic system of equations:

$$\mathbf{Kd} = \mathbf{f} \tag{2.7}$$

with the stiffness matrix given by

$$\mathbf{K} = \int_{\Omega^h} \mathbf{B^T D B} d\Omega \tag{2.8}$$

and the load vector by

$$\mathbf{f} = \int_{\Omega^h} \mathbf{N^T b} d\Omega + \int_{\Gamma_t} \mathbf{N^T} \bar{\mathbf{t}} d\Gamma \tag{2.9}$$

where Ω_h is the discretized domain, formed by the union of elements Ω_e. The stiffness matrix $\mathbf{K}$ is symmetric, positive definite and with a strain-displacement matrix defined

as

$$\mathbf{B}_i(\mathbf{x}) = \bigtriangledown_s N_i(\mathbf{x}) = \begin{bmatrix} \frac{\partial N_i}{\partial x} & 0 \\ 0 & \frac{\partial N_i}{\partial y} \\ \frac{\partial N_i}{\partial y} & \frac{\partial N_i}{\partial x} \end{bmatrix} \tag{2.10}$$

where, i in Eq. (2.10) is an arbitrary node of the element. The size of the $\mathbf{B}$ matrix depends on the number of nodes in an element. The finite element literature seldom shows systematic ways to extend element formulation technology beyond quadrilaterals. The Finite Element stiffness matrix given in equation (2.8) must be evaluated over the element. In conventional finite element method an element does not have more than four edges for 2D domains. In general, the Gau$\mathcal{B}$ quadrature rule can be effectively used to integrate the weak forms. To integrate weak forms over the *n-gon*, no general quadrature rule is available which have optimal ways to choose its accuracy. The following three methods can be used for integration of weak form over the *n-gon* element.

1. The method given by Sukumar and Tabarraei [10] is used to integrate over the *n-gon* element. In this method a physical element is mapped to a canonical domain and then the element is subdivided into n triangles and then the well known rules are applied on a triangle for numerical integration. This method involves two levels of isoparameric mapping: Physical element $(\Omega_e) \rightarrow (\Omega_o) \rightarrow$Triangle. The standard triangular quadrature rule is used for integration over the triangle. More over in isoparametric mapping the length measures are preserved, but not the bounds of included angles,and so the positivity of the Jacobian needs to be ensured additionally. To ensure the positivity of the Jacobian, the element should be a convex element in this approach.

2. Another method to integrate over the *n-gon* element is the Smoothed Finite Element Method (SFEM) [16], which is based on strain smoothening, introduced by Chen[18] for mesh-free methods. The extension of strain smoothening approach to finite element method leads to integration on boundary of the finite elements, which avoids the requirement of isoparametric mapping. Even in case of the SFEM, the *n-gon* element is subdivided into n triangles, solely for the purpose of numerical

integration. Unlike in the triangulation scheme, the integration points lie on the boundary of the triangles.

3. The other potential solution to integrate over the *n-gon* element is the method developed by Sundarrajan *et al* [11]. In this method an *n-gon* element is mapped to a unit disk using conformal mapping and various cubature rules can be used for integration.

In this work this third method is used to integrate over the *n-gon* element. Mapping is done using SCPACK [15] subroutines in FORTRAN.

2.1 Schwarz-Christoffel Conformal Mapping

In this section, we describe the method to map an arbitrary *n-gon* to a unit disk using Schwarz-Christoffel conformal mapping (SCCM) and a few numerical integration rules for 2-dimensional cases.

An important family of conformal maps has its roots in complex analysis. A conformal map f (angle preserving) of a region in the complex plane is an analytic (smooth) function whose derivative vanishes within the region[15]

Definition: If $U \subset \mathbb{C}$, then a function $f\colon U \to \mathbb{C}$ is conformal, if and only if it is analytic and its derivative is nonzero in U.

Any simply connected domain in the plane with a boundary containing more than one point can be conformally mapped onto the interior of a disk. Since the real physical domain and the complex domain are isomorphic, there exists a bijective map (i.e. one to one and onto) between the two, such that both the map and its inverse are structure preserving. This follows from the following theorem:

Theorem: If U is a simply connected open subset of the complex plane $\mathbb{C}$, then there exists a bijective mapping $f : U \to A$ where, $(A = z \in \mathbb{C}\colon |z| < 1)$ is the open unit disk

The basic Schwarz-Christoffel formula [15] is a recipe for a conformal map f from the complex upper half plane to the interior of a polygon. The polygon may have cracks or vertices at infinity, its vertices are denoted by $w_1, w_2, \cdots, w_n$ and the numbers

$\alpha_1\pi, \alpha_2\pi, \cdots, \alpha_n\pi$ are the interior angles at the vertices. The pre-images of the vertices are real and are denoted by $z_1 < z_2 < z_3 < \cdots < z_n = \infty$. The Schwarz-Christoffel map f is given by

$$f(z) = A \int^z \prod_{j=1}^{n} (z' - z_j)^{-\beta_j}\, dz' + B \tag{2.11}$$

In this equation z is the independent complex variable in the upper half-plane, the z_j are the "pre-vertices", i.e., points on the real axis which are preimages of the corners $w_j = f(z_j)$ of the polygon, the α_j are $1/\pi$ times the interior angles at those corners, and A and B are two complex constants.

The Schwarz-Christoffel transformation therefore maps the upper half-plane onto a polygonal region with interior angles $\alpha_j\pi$. If ∞ is a prevertex or preimage, the vertices are rotated so that $f(\infty) = w_n$, then the product has the upper limit $n - 1$. The lower integration limit is left unspecified as it could be chosen arbitrarily in the upper half-plane H^+, which implies, any path from the lower limit to z could be chosen which lies inside H^+.

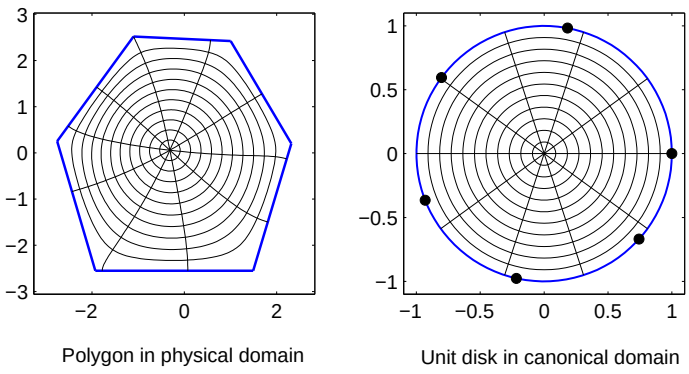

Figure 2.1: Mapping convex polygon from physical domain to unit disk in canonical domain. Vertices of the polygon are represented as dark circles in the unit disk.

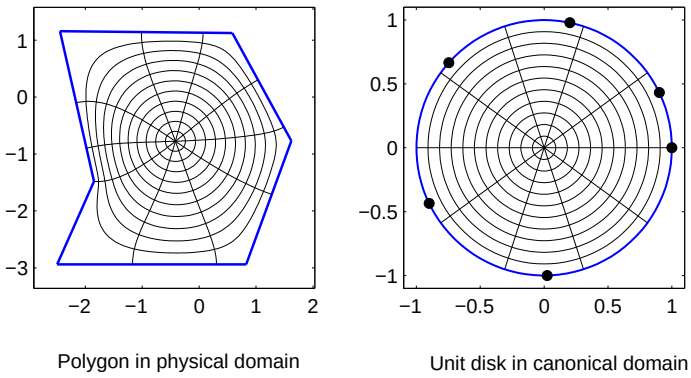

Figure 2.2: Mapping concave polygon from physical domain to unit disk in canonical domain. Vertices of the polygon are represented as dark circles in the unit disk.

Conformal maps can also be found between domains which are not simply connected. Figure 2.1 shows a conformal mapping of an arbitrary polygon onto a unit disk. The mapping is made with respect to a point in the complex plane, which forms the *conformal center*. Either the geometric center is specified as conformal center, or it can be user specified so that the user has control on distribution of integration points. The exact solution to the integral Eq. (2.11) is available for very few class of problems. Eqs. (2.12) and (2.13) give a conformal mapping function for a triangle and a square respectively. A mapping to a plane triangle with angles πa, πb and $\pi(1-a-b)$ is given by

$$z = f(\varsigma) = \int^{\varsigma} \frac{dw}{(w-1)^{1-a}(w+1)^{1-b}} \tag{2.12}$$

And the upper half-plane is mapped to the square by

$$z = f(\varsigma) = \int^{\varsigma} \frac{dw}{\sqrt{w(w^2-1)}} \tag{2.13}$$

In a similar way, the upper half-plane can be mapped to any arbitrary *n-gon*. Likewise, any arbitrary polygon can be mapped onto a unit disk. Figure (2.1) shows the conformal mapping of a concave polygon to a unit disk. For problems with more vertices, unless the polygon is symmetric, in general the SCCM integral in Eq.(2.11) has no closed form solution [14]. In such cases, the SCCM involves the following three numerical steps:

1. Finding points z_k, known as parameter problem; these unknown parameters can be found by solving a system of nonlinear equations that assert that the side length of the *n-gon* are correct;

2. Calculating the SCCM integral in Eq.(2.11), integrals can be evaluated by a *Compound Gauß Jacobi quadrature* rule.

3. Inverting the map. Map inversion can be evaluated by a Newton iteration. All these numerical steps are implemented in FORTRAN using SCPACK subroutines [15].

Let the conformal mapping from a unit disk to a polygon be defined by

$$w = f(z) \tag{2.14}$$

In case of the proposed method, the polygon is first mapped on to a unit disk. This is done by computing the inverse of the map given by Eq.(2.14). And the inverse is computed by inverting the Schwarz Christoffel formula

$$\frac{df(z)}{dz} = A\left(z' - z_j\right)^{-\beta_j} \tag{2.15}$$

to yield a formula

$$\frac{dz}{df(z)} = \frac{1}{A}\left(z' - z_j\right)^{\beta_j} \tag{2.16}$$

Remark: This inversion is possible because the method relies on conformal map, which means $\left|\frac{df(z)}{dz}\right| > 0$ everywhere.

Since a map is involved, the computation of the Jacobian associated with this transformation is required and computed in the following manner. If r is the radius of the canonical domain, then

$$\frac{\partial w}{\partial x} = \frac{\partial w}{\partial r}\frac{\partial r}{\partial x}, \qquad \frac{\partial w}{\partial y} = \frac{\partial w}{\partial r}\frac{\partial r}{\partial y}. \tag{2.17}$$

In the canonical domain, the value of r is computed as $r^2 = \xi^2 + \eta^2$. The derivative with respect to the spatial coordinates, X and Y, is given by

$$\begin{bmatrix} \frac{\partial r}{\partial X} \\ \\ \frac{\partial r}{\partial Y} \end{bmatrix} = \begin{bmatrix} \frac{\partial \xi}{\partial X} & \frac{\partial \eta}{\partial X} \\ \\ \frac{\partial \xi}{\partial Y} & \frac{\partial \eta}{\partial Y} \end{bmatrix} \begin{Bmatrix} \frac{\xi}{r} \\ \\ \frac{\eta}{r} \end{Bmatrix} \tag{2.18}$$

The mapping done using Eq.(2.18) assumes both the physical domain and the canonical domain (unit disk) as imaginary planes. Let the physical domain be represented by (x, y) and the canonical domain by (ξ, η). Let $z = (\xi + i\eta)$ and because of the iso-morphic property, we can write the mapping in complex form as $f(z) : (\xi + i\eta) \mapsto (x + iy)$. From complex analysis [**?**], we have

$$\frac{df}{dz} = f'(z) = \frac{\partial x}{\partial \xi} + i\frac{\partial y}{\partial \xi} = \frac{\partial y}{\partial \eta} - i\frac{\partial x}{\partial \eta} \tag{2.19}$$

And, from Eq.(2.19), the mapping can be defined by the following expression

$$\begin{bmatrix} \frac{\partial r}{\partial x} \\ \\ \frac{\partial r}{\partial y} \end{bmatrix} = \begin{bmatrix} \frac{\partial \xi}{\partial x} & \frac{\partial \eta}{\partial x} \\ \\ \frac{\partial \xi}{\partial x} & \frac{\partial \eta}{\partial x} \end{bmatrix} \begin{Bmatrix} \frac{\xi}{r} \\ \\ \frac{\eta}{r} \end{Bmatrix} = [J]^{-1} \begin{bmatrix} \frac{\xi}{r} \\ \\ \frac{\eta}{r} \end{bmatrix} \tag{2.20}$$

This procedure can be used to compute the Jacobian. In the proposed method, there is only one level of mapping.

Remark: In the conformal mapping, $\left|\frac{df(z)}{dz}\right| > 0$ everywhere and the mapping preserves the included angle of the *n-gon*. Hence, the Jacobian is always positive irrespective of

convexity.

2.2 Numerical Integration Rule

Once the mapping of an n-gon element onto unit disk is done using Schawrz-Christoffel conformal mapping, then integration is carried on unit disk. The integration points are obtained by employing cubature rules on a circle. These integration points are then mapped onto the parent n-gon using SCCM formula given in Eq. (2.16). Various cubature rules on a circle are given in this section.

2.2.1 Midpoint Quadrature Rule

In this method [19] the unit disk is divided into concentric circles and radial lines, then a midpoint quadrature rule is applied for the area of the subdomains in the interior of the disk. The integral is evaluated on each of the centroid of the subdomains as the area of the subdomain multiplied by the integrand evaluated at the centroid of the subdomain. The following approximation can be used to integrate $f(x, y)$ on a disk Ω of radius R_o:

$$\int_{\Omega} f(x,y)dxdy \simeq \sum_{i=1}^{n_\theta}\sum_{j=1}^{n_r} A_{ij} f(r_j \cos\theta_i, r_j \sin\theta_i) \tag{2.21}$$

where n_θ is the number of sectors in which the disk is partitioned and n_r is the number of radial sub-divisions. Here,

$$r_j = \frac{j^2 - j + 1/3}{j - 1/2}\Delta r; \qquad \theta_i = (i - 1/2)\Delta\theta \tag{2.22a}$$

$$\Delta r = \frac{R_o}{n_r}; \quad \Delta\theta = \frac{2\pi}{n_\theta}; \qquad A_{ij} = (j - \frac{1}{2})\Delta\theta(\Delta r)^2 \tag{2.22b}$$

Where,r and *theta* are the polar coordinates.

Gauß Chebyshev Rule

Peirce([17]) in his book provides an arbitrary polynomial accuracy of degree $n = 4m+3$, $m = 0, 1, 2, \cdots$, in $x = r\cos\theta$ and $y = r\sin\theta$, where following approximation can be used to evaluate the integral

$$\int\int_{\Omega} f(x,y)dxdy \simeq \sum_{i=1}^{4(m+1)} \sum_{j=1}^{m+1} A_{ij} f(r_j \cos\theta_i, r_j \sin\theta_i) \tag{2.23}$$

where

1. $\theta_i + 1 - \theta_i = \frac{2\pi}{k+1}$, $i = 1, 2, \cdots 4(m+1)$
2. $A_{ij} = \frac{\pi}{4(m+1)P_{m+1}{}'r_j^2} \int_0^{R_0^2} \frac{P_{m+1}r^2}{r^2 - r_j^2} dr^2$, $j = 1, 2, \cdots, m+1$
3. r_i^2 are the $m+1$ zeros of $P_{m+1}(r^2)$, the Legendre polynomial in r^2 of degree $m+1$, orthogonalized on $[0, R_o^2]$.

Since Gauß-Chebyshev quadrature automatically arises in the θ direction, the integration points are on equally spaced an radial lines and the weights are independent of their angular positions.

Gauß Legendre Rule

The Gauß Legendre product rule on a unit disk is given by

$$\int\int_{\Omega} f(x,y)dxdy = \int_{y=-R_o}^{R_o} \int_{x=-X(y)}^{X(y)} f(x,y)dxdy \simeq \sum_{i=1}^{N_x} \sum_{j=1}^{N_y} A_{ij} f(x_i, y_j) \tag{2.24}$$

where,

N_x and N_y are the number of integration points chosen along the x- and y- directions,respectively,

$A_{ij} = W_i^x W_j^y$ is the product of the usual Gaussian weights.

The Gauß integration can be applied by transforming the original coordinate system

(r, θ) to the natural coordinate system (s, t) via isoparametric formulation. The center of the local coordinate system (s, t) can be expressed as

$$r_m = \frac{1}{2}(r_1 + r_2) \tag{2.25a}$$

$$\theta_m = \frac{1}{2}(\theta_1 + \theta_2) \tag{2.25b}$$

Corresponding map is

$$s = \frac{2(r - r_m)}{r_2 - r_1} = \frac{\left(r - \frac{r_1 + r_2}{r_2 - r_1}\right)}{r_2 - r_1} \tag{2.26a}$$

$$t = \frac{2(\theta - \theta_m)}{\theta_2 - \theta_1} = \frac{\left(\theta - \frac{\theta_1 + \theta_2}{\theta_2 - \theta_1}\right)}{\theta_2 - \theta_1} \tag{2.26b}$$

The Jacobian matrix becomes

$$|J| = \begin{vmatrix} \frac{\partial r}{\partial s} & \frac{\partial \theta}{\partial s} \\ \frac{\partial r}{\partial t} & \frac{\partial \theta}{\partial t} \end{vmatrix} = \begin{vmatrix} \frac{r_2 - r_1}{2} & 0 \\ 0 & \frac{\theta_2 - \theta_1}{2} \end{vmatrix} = \frac{1}{4}(r_2 - r_1)(\theta_1 - \theta_2) \tag{2.27}$$

The original equation is transformed into isoparametric form as

$$\int_{\theta_1}^{\theta_2} \int_{r_1}^{r_2} \mathbf{B}(r, \theta) \mathbb{D} \mathbf{B}(r, \theta) dr d\theta = \int_{-1}^{+1} \int_{-1}^{+1} \mathbf{B}(s, t) \mathbb{D} \mathbf{B}(s, t) |J| ds dt \tag{2.28}$$

where $|J|$ is given by (2.27). Therefore, the numerical integration takes the form

$$\int_{\theta_1}^{\theta_2} \int_{r_1}^{r_2} \mathbf{B}(r, \theta) \mathbb{D} \mathbf{B}(r, \theta) dr d\theta = \sum_{i=1}^{N_x} \sum_{j=1}^{N_y} A_{ij} \mathbf{B}(s_i, t_j) \mathbb{D} \mathbf{B}(s_i, t_j) \frac{1}{4}(r_2 - r_1)(\theta_1 - \theta_2) \tag{2.29}$$

In case of the proposed method, the physical element is mapped onto a unit disk using the SCCM and one of the above numerical integration rule can be adopted to numerically integration the Eq. (5.12). The numerical integration for midpoint quadrature rule is

given by

$$\mathbf{K} = \int_{\Omega^h} \mathbf{B}^T \mathbb{D}\mathbf{B} = \int_{\theta_1}^{\theta_2} \int_{r_1}^{r_2} \mathbf{B}(r,\theta)\mathbb{D}\mathbf{B}(r,\theta) dr d\theta \tag{2.30a}$$

$$\simeq \sum_{i=1}^{n_\theta} \sum_{j=1}^{n_r} A_{ij} \mathbf{B}(r_j \cos\theta_i, r_j \sin\theta_i)\mathbb{D}\mathbf{B}(r_j \cos\theta_i, r_j \sin\theta_i)|J| \tag{2.30b}$$

where $|J|$ is the determinant of the Jacobian matrix for the conformal mapping, given by Eq. (2.20). Once the integration points are computed on a unit disk using one of the above methods, an affine transformation is performed to obtain the integration points on the physical domain.

The location of the integration points after mapping to physical element is shown in the figure 2.3.

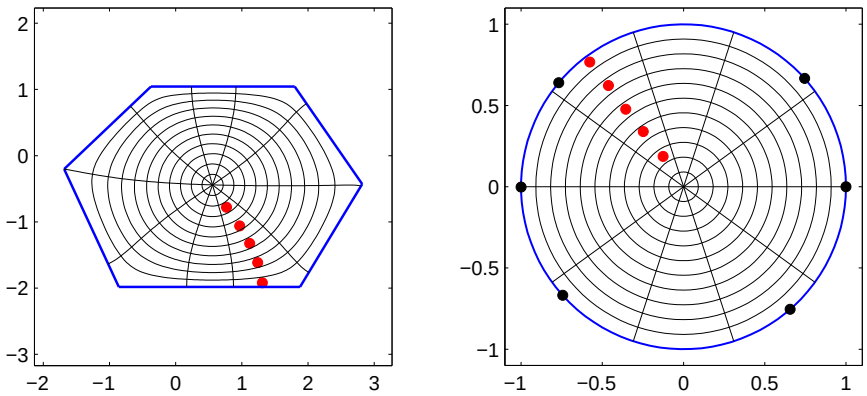

Figure 2.3: Location integration points on the physical element and corresponding location of the integration points on the unit disk in the canonical domain.

In this chapter mapping of an n-gon element from physical domain to a unit disk in the

canonical domain based on Schwarz-Christoffel conformal mapping is given. Integration of a function $f(x, y)$ over the polygon is done after mapping the polygon to the unit disk, and then various cubature rules to integrate over the unit disk is applied. This method of integration is used in this work to integrate the weak form of the governing equation and thus stiffness matrix. In this work Midpoint cubature rule is taken to integrate over the unit disk.

Chapter 3

Interpolation Functions For Polygonal Element

In chapter 2 numerical integration of weak form of governing equation on polygon based on Schwarz-Christoffel conformal mapping, basics of Schwarz-Christoffel conformal mapping have been explained. As there involves a mapping, there is exist a jacobian. Deriving the jacobian of the mapping is also given in the same chapter. Cubature rules to integrate over the unit disk were explained. This chapter is devoted for the construction of interpolation functions for polygonal elements. Various methods for constructing interpolation function for polygonal element are given in this chapter.

3.1 Interpolation Functions

In standard Finite Element Method, which uses isoparametric mapping, interpolation functions are constructed on master element. To use polygonal element, interpolation functions are required to be constructed on the polygon element. And these interpolation function should satisfy the following properties:

1. Non-negative ness, $0 \leq N_i(\mathbf{x}) \leq \mathbf{1}$

2. Interpolation of nodal data, $N_i(\mathbf{x_j}) = \delta$

3. Partition of unit $\sum_{i=1}^{n} = 1$

4. Linear completeness, $N_i(\eta)\mathbf{x_i} = \mathbf{x}(\eta)$.

5. Smooth with in the domain.

   Here N is the shape function.

The triangle and the quadrilateral are basic element shapes used in most two-dimensional finite element methods. In general, if polygonal elements with more than four vertices are available,which is new in any finite element computations, then it could significantly reduce the problem of complex mesh, gradient errors and shape-sensitivity etc. The removal of this restriction that domain can have n-gon shape has the potential to lead to new developments in mesh generation and the finite element method. Polygonal finite elements provide greater flexibility for the meshing of complex geometries, are potentially useful for the modeling of polycrystalline materials, can serve as transition elements in finite element meshes and are well suited for material design.

3.1.1 Conforming Interpolants On Polygons

Consider a polygonal domain $\Omega \subset \mathbf{R}^2$ that is described by n nodes. Let ith node be p_i and coordinate of vertex-node i is $\mathbf{x}_i = (x_i, y_i)$. Any point p with coordinate $\mathbf{x} = (x, y) \in \bar{\Omega}$, has a set of associated shape functions ϕ_i $(\mathbf{x})$. An interpolation scheme for a scalar valued function $u : \bar{\Omega} \rightarrow \mathbf{R}$ can be written as

$$u^h(\mathbf{x}) = \sum_{i=1}^{n} \phi_i(\mathbf{x}) u_i$$

where u_i are the unknowns at the n neighbors of point p. To use C^0 shape functions, the interpolant u^h should satisfy the following properties:

1. Applying the partition of unity to assure constant precision, and that $\phi_i(\mathbf{x})$ is non

negative and bounded, one has

$$\sum_{i=1}^{n} \phi_i(\mathbf{x}) = 1, \quad 0 \leq \phi_i(\mathbf{x}) \leq 1$$

2. Interpolate nodal data:

$$\phi_i(\mathbf{x}) = \delta_{ij}$$

where δ_{ij} is the Kronecker-delta. It states that the interpolated displacement at a node recovers the nodal data: $u^h(\mathbf{x}) = u_i$.

3. Linear precision or linear completeness:

$$\sum_{i=1}^{n} \phi_i(\mathbf{x})\mathbf{x}_i = (\mathbf{x})$$

From the above property, it can be concluded that the shape function can exactly reproduce a linear function.

4. The shape function $\phi_i \in C^\infty$ within the domain. Along the edges of the polygon, the interpolant must be piece-wise linear (C^0 function), that is

$$u^h(t) = tu_1 + (1-t)u_2, \;\; \mathbf{x} = t\mathbf{x}_1 + (1-t)\mathbf{x}_2, \;\; \mathbf{x} \in \partial\Omega, \;\; t \in [0,1].$$

The following methods can be used to build shape functions on a polygonal domain.

1. Shape functions using length and area measures [20],[10],[22],[21] (Like Wachpress shape function, Metric coordinate, Rational Polynomial).

2. Natural neighbor shape function [25], [26], [23].

3. Maximum entropy approximant [24].

4. Barycentric coordinates on irregular *n-gon* [27],[28].

In this work, Wachspress shape functions are used to construct interpolation function on an n-gon element, as this satisfies the requirement of a interpolation function given section 3.1.1.

3.1.2 Wachspress shape functions

Using the principles of projective geometry, Wachpress constructed rational basis functions on polygonal domain. In this the algebraic equations of the edges are used to ensure nodal interpolation and linearity on the boundaries. Wachpress proved that for an *n-gon* these shape functions are rational polynomials. In general, for an n-sided convex polygon, a Wachpress shape function $N_i^{(n)}(x, y)$ is a polynomial of the following form:

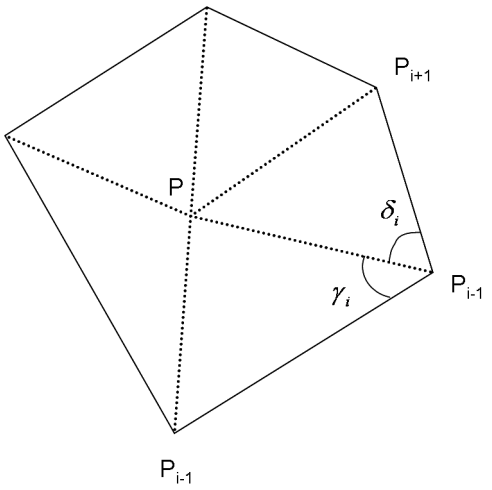

Figure 3.1: Barycentric coordinates: P_i, P_{i-1} and P_{i+1} are the vertices of polygon. P is the point in the polygon.

$$N_i^n(x, y) = \frac{\mathcal{P}^{n-2}(x, y)}{\mathcal{P}^{n-3}(x, y)} \tag{3.1}$$

$\mathcal{P}^{(m)}(x, y)$: m-degree polynomial in x, y

Wachspress shape functions have the following essential features:

- Each function is positive in the convex domain
- Each function is linear on each side of the convex n-gon

- The set of functions exactly interpolates an arbitrary linear field

In [30], a simple expression is obtained for Wachspress's basis function, which can be written as

$$\phi_i^w(\mathbf{x}) = \frac{w_i(\mathbf{x})}{\sum_{j=1}^{n} w_j(\mathbf{x})}, \tag{3.2a}$$

$$w_i(\mathbf{x}) = \frac{A(p_{i-1}, p_i, p_{i+1})}{A(p_{i-1}, p_i, p)A(p_i, p_{i+1}, p)} = \frac{\cot\gamma_i + \cot\delta_i}{||\mathbf{x} - \mathbf{x}_i||^2} \tag{3.2b}$$

where the last expression is due to Meyer *et al* [30]. In (3.2) $A(a, b, c)$ is the signed area of triangle $[a, b, c]$ and γ_i and δ_i are shown in figure (3.1.2). We infer from (3.2) that for $\phi_i^w(\mathbf{x})$ to be non-negative, the polygon must be convex ($\gamma_i + \delta_i < \pi$). The angles γ_i and δ_i are not explicitly computed, instead the vector cross and dot product formulae are used to compute the cotangents. For instance, if the coordinates of the vertices of the triangle $[p_i, p_{i+1}, p]$ be (a_1, a_2), (b_1, b_2), and (c_1, c_2), respectively, then

$$\cot\delta_i = \frac{(p_{i+1} - p_i) \cdot (p - p_i)}{|(p_{i+1} - p_i) \times (p - p_i)|} \tag{3.3a}$$

$$= \frac{(b_1 - a_1)(c_1 - a_1) + (b_2 - a_2)(c_2 - a_2)}{(b_1 - a_1)(c_2 - a_2) - (c_1 - a_2)(b_2 - a_2)} = \frac{C}{S} \tag{3.3b}$$

and its derivatives are

$$\frac{\partial(\cot\delta_i)}{\partial c_1} = \frac{(b_1 - a_1) - \cot\delta_i(a_2 - b_2)}{S}, \tag{3.4a}$$

$$\frac{\partial(\cot\delta_i)}{\partial c_2} = \frac{(b_2 - a_2) - \cot\delta_i(b_1 - a_1)}{S}. \tag{3.4b}$$

A similar procedure is adopted to compute $\cot\gamma_i$ that appears in (3.2). The Wachspress shape functions are the lowest order shape functions that satisfy boundedness, linearity and linear dependence on convex polyshapes [29]. In the figure 3.2 shows shape function for a hexagon with Finite Element model placed at vertices.

Construction of interpolation function for polygonal element by various methods was given in this chapter. In this work Wachspress shape function is used interpolation

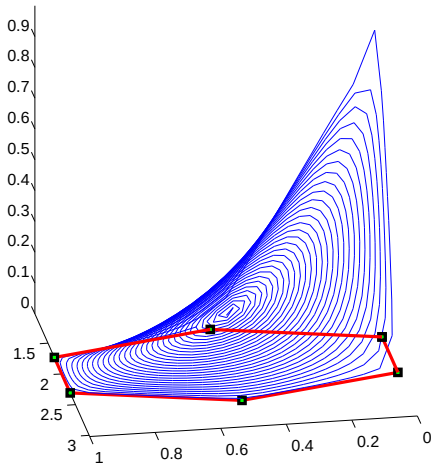

Figure 3.2: Wachspress shape function N_i for i^{th} node on a hexagon

function for polygonal element. Wachspress shape functions satisfies the requirements of an interpolation function given in section 3.1.1. Therefore, Wachspress shape function is used as interpolation function in this work. Using the Wachspress shape function and integration technique given in chapter 2 few bench mark problems like static and free-vibration analysis of a cantilever beam are solved. The same method is also extended to linear elastic fracture mechanics using polygonal element based on Schawrz-Christoffel conformal mapping and overall convergence of the method is studied in the subsequent chapters.

Chapter 4

Static and Free Vibration Analysis Using Poly-Schwarz Christoffel Conformal Mapping-FEM

In chapter 2 a new integration technique to integrate the weak form of governing equation over the polygonal element has been explained. And in chapter 3 construction of interpolation function on the polygonal element has been explained. Using this new integration technique and interpolation function few bench mark problems like static and free-vibration problem of a cantilever beam is solved and the overall convergence of the method is examined in this chapter.

4.1 Static Analysis

4.1.1 Governing Equations and weak form

The governing equations and weak form for the static analysis is given in chapter 2 from Eq. (2.1) to Eq. (2.7).

4.1.2 Equilibrium Patch Test

To study the accuracy of the proposed method equilibrium patch test is performed. Considering a uniaxial stress $\sigma = 6.894757\ kPa$ (1 Psi) under the condition of plane stress applied in y direction on top of the unit square while essential boundary conditions are applied at the bottom edge as shown in figure 4.2. The exact displacement [31] is given as

$$u(x, y) = \frac{\nu}{E}(1 - x). \tag{4.1a}$$

$$v(x, y) = \frac{y}{E}. \tag{4.1b}$$

$$R.E_d = \sqrt{\frac{\int_\Omega (u^h - u^{exact})^2 d\Omega}{\int_\Omega (u^{exact})^2 d\Omega}} \tag{4.2}$$

The polygonal mesh shown in Figure 4.1 is considered for the patch test. The relative error in displacement norm Eq. (4.2) is (L_2) is given in table 4.1. From this patch test it can be concluded that the method converges as mesh is refined to fine mesh.

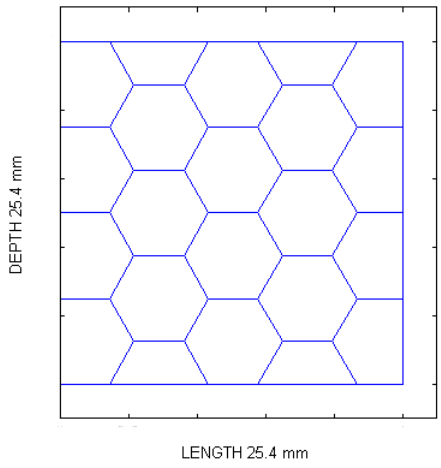

Figure 4.1: Polygonal mesh used for patch test. The domain is dicretized using hexagonal elements.

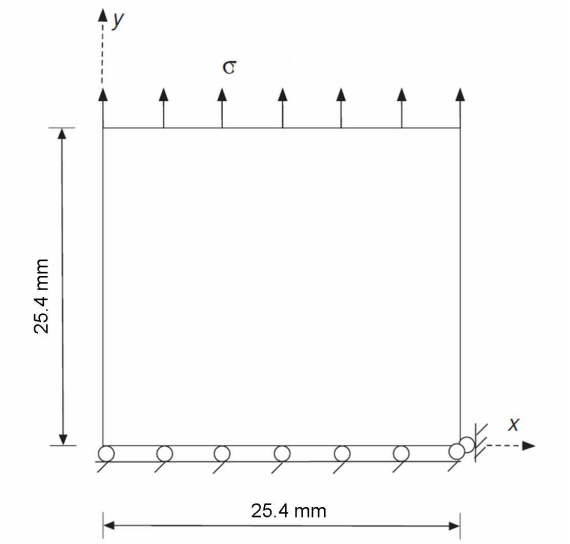

Figure 4.2: Geometry, loading and boundary conditions used for patch test. Far field stress $\sigma = 6.894757\ kPa$ $(1Psi)$ is applied.

Table 4.1: Relative error in displacement norm (Re_d) Eq. (4.2)

Number of nodes	Re_d
46	1.666×10^{-3}
154	5.133×10^{-5}
628	5.607×10^{-5}
944	5.380×10^{-6}

4.1.3 Bending Of Thick Cantilever Beam

A thick cantilever two-dimensional beam, having dimensions $L = 10$, $D = 2$ and $B = 1$, subjected to parabolic shear equal to 100 at free end is examined for convergence study. Young's modulus of the material is equal to 3X10e7 and Poisson's ratio is equal to 0.3 is taken. Geometry, loading and boundary conditions are shown in figure 4.3. The exact

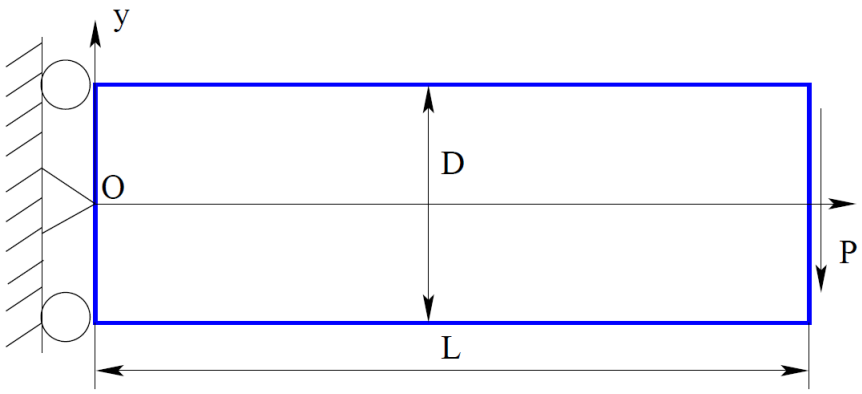

Figure 4.3: Geometry, loading and boundary conditions of thick cantilever beam used for convergence study.

solution for displacements and stresses is available in Timoshenko and Goodier [32] and given by:

$$u(x,y) = \frac{Py}{6\overline{E}I}\left[(6L-3x)x + (2+\overline{\nu})(y^2 - \frac{D^2}{4})\right] \tag{4.3a}$$

$$v(x,y) = -\frac{P}{6\overline{E}I}\left[3\overline{\nu}y^2(L-x) + (4+5\overline{\nu})\frac{D^2x}{4} + (3L-x)x^2\right] \tag{4.3b}$$

where I, the moment of inertia (second moment of area) is given by: $I = D^3/12$ and $\overline{E}$ and $\overline{\nu}$ in 4.3 are given by

$$\overline{E} = \begin{cases} E \ \text{(plane stress)}, \\ \frac{E}{1-\nu^2} \ \text{(plane strain)} \end{cases} \qquad \overline{\nu} = \begin{cases} \nu \ \text{(plane stress)}, \\ \frac{\nu}{1-\nu} \ \text{(plane strain)} \end{cases}$$

The stresses corresponding to the displacements in (4.3) given by

$$\sigma_{xx}(x,y) = \frac{P(L-x)y}{I} \tag{4.4a}$$

$$\sigma_{yy}(x,y) = 0 \tag{4.4b}$$

$$\sigma_{xy}(x,y) = -\frac{P}{2I}\left(\frac{D^2}{4} - y^2\right) \tag{4.4c}$$

For this problem structured hexagonal mesh is developed. Convergence study has been performed by increasing the number of elements. Relative error in displacement norm and energy norm has been studied. Figure 4.5 shows the convergence of relative error in displacement norm. It has been observed that the method converges to the exact solution as number of elements increased.

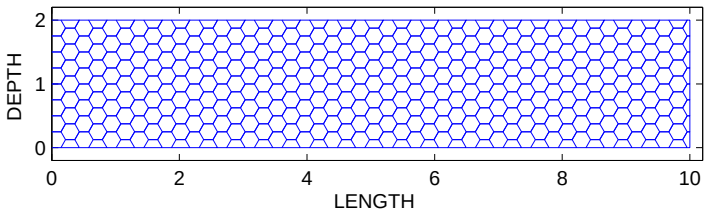

Figure 4.4: Domain discretization of cantilever beam with structured hexagonal mesh.

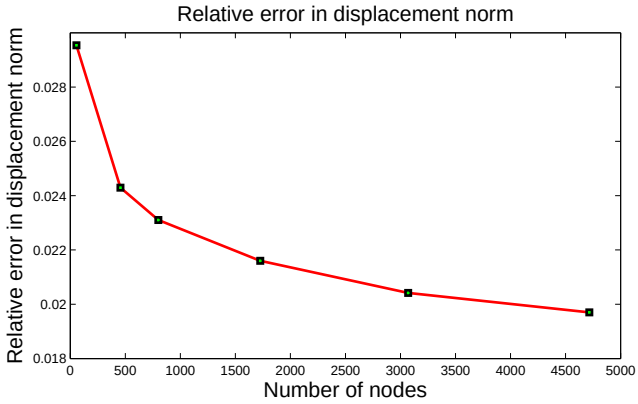

Figure 4.5: Convergence in the Relative error in displacement norm Eq. (4.2) for the cantilever beam with structured hexagonal mesh.

4.2 Free Vibration Analysis

4.2.1 Governing Equations and weak form

The governing equilibrium equations for a 2D dynamic problem defined in the domain Ω

$$\nabla_s^{\mathrm{T}}\boldsymbol{\sigma} + \mathbf{b} = \rho\ddot{\mathbf{u}} \quad \text{in } \Omega \tag{4.5}$$

Where $\mathbf{0}$ is a null vector, $\boldsymbol{\sigma}$ is the stress tensor and $\mathbf{b}$ is the vector of external forces. The following are the prescribed boundary conditions

$$\mathbf{u} = \overline{\mathbf{u}} \ \textit{in} \ \Gamma_u \tag{4.6}$$

$$\mathbf{n}^T\boldsymbol{\sigma} = \overline{\mathbf{t}} \ \textit{on} \ \Gamma_t \tag{4.7}$$

where $\overline{\mathbf{u}} = (\overline{u}_x, \overline{u}_y)^T$ is the prescribed displacement vector on the essential boundary Γ_u;

$\mathbf{t} = (\bar{t}_x, \bar{t}_y)^T$ is the prescribed traction vector on the natural boundary Γ_t; $\mathbf{n}$ is the unit outward normal vector. where ρ is the mass density. The discrete equations for the

dynamic problem are generated from the Galerkin weak form

$$\int (\delta \mathbf{u})^T \rho(\ddot{\mathbf{u}}) d\Omega - \int_\Omega (\bigtriangledown_s \delta \mathbf{u})^T \mathbb{D} (\bigtriangledown_s \delta \mathbf{u}) d\Omega - \int_\Gamma (\delta \mathbf{u}^T) \mathbf{b} d\Omega - \int_\Gamma (\delta \mathbf{u})^T \bar{\mathbf{t}} d\Gamma = 0 \quad (4.8)$$

The Polygonal finite element method uses the following trial and test functions:

$$\mathbf{u}^h(\mathbf{x}, t) = \sum_{i=1}^{NP} \mathbf{N}_i(\mathbf{X}) \mathbf{d}_i(t), \quad \delta \mathbf{u}^h(\mathbf{x}) = \sum_{i=1}^{NP} \mathbf{N}_i(\mathbf{X}) \delta \mathbf{d}_i \quad (4.9)$$

By substituting the approximations, $\mathbf{u}^h$ and $\delta \mathbf{u}^h$, into the weak form and invoking the arbitrariness of virtual nodal displacements, Eq. (4.8) yields the standard discretized algebraic system of equations:

$$\mathbf{M}\ddot{\mathbf{d}} + \mathbf{K}\mathbf{d} = \mathbf{f} \quad (4.10)$$

with the mass and stiffness matrix given by

$$\mathbf{M} = \int_{\Omega^h} \mathbf{N}^\mathbf{T} \rho \mathbf{N} d\Omega, \quad \mathbf{K} = \int_{\Omega^h} \mathbf{B}^\mathbf{T} \mathbf{D} \mathbf{B} d\Omega \quad (4.11)$$

and the load vector by

$$\mathbf{f} = \int_{\Omega^h} \mathbf{N}^\mathbf{T} \mathbf{b} d\Omega + \int_{\Gamma_t} \mathbf{N}^\mathbf{T} \bar{\mathbf{t}} d\Gamma \quad (4.12)$$

where Ω_h is the discretized domain, formed by the union of elements Ω_e. For free vibration load vector $\mathbf{f} = \mathbf{0}$. Therefore, equation (4.10) becomes

$$\mathbf{M}\ddot{\mathbf{d}} + \mathbf{K}\mathbf{d} = \mathbf{0} \quad (4.13)$$

Assuming the modal solution:

$$d(t) = \sum \hat{d}(\omega) e^{i\omega t} \quad (4.14)$$

And substituting Eq.(4.14) in Eq. (4.13) we get

$$\mathbf{K}\hat{d} = \omega^2 \mathbf{M}\hat{d} \quad (4.15)$$

Eq.(4.15) is the eigen value problem which is solved for least natural frequency. In this work Jacobi method is used to solve the Eq. (4.15).

4.2.2 Free Vibration Of Thin Cantilever Beam

A thin cantilever two-dimensional beam, having dimensions $L = 100$, $D = 1$ and $B = 1$, is examined for free vibration problem. Young's Modulus of the material is equal to 3×10^7 and Poisson's ratio equal to 0.3 is taken. Convergence of relative error in natural frequency is shown in figure 4.6. From this plot it can be concluded that method converges to analytical natural frequency as number of nodes increases. Therefore, the new integration scheme [11] based on Schwarz-Christoffel conformal mapping works fine for the free vibration problem also.

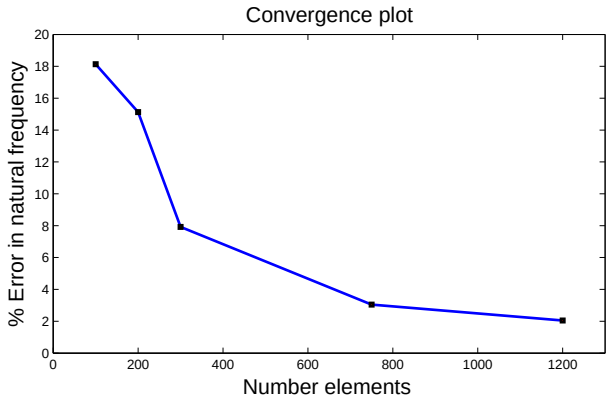

Figure 4.6: Convergence of Relative error in natural frequency for thin cantilever beam.

4.2.3 Free Vibration Of Thick Cantilever Beam

For this case, convergence is examined for

1. Rectangular elements.

2. Structured Polygonal elements.

A thick cantilever two-dimensional beam, having dimensions $L = 10$, $D = 2$ and $B = 1$, is examined for free vibration problem. Young's Modulus of the material is equal to

3×10^7 and Poisson's ratio equal to 0.3 is taken. In this work convergence of normalized L_2 norm given in Eq. (4.16) for natural frequency with number of nodes for the thick cantilever beam is studied and convergence plot is shown if figure 4.7. Convergence of the normalized L_2 norm is shown both for the rectangular elements and hexagonal elements. As the number of nodes increases, the normalized L_2 norm converges. Therefore, the method converges for free vibration problem and thus the new integration scheme works fine for the free-vibration problem (Eigen value problem). Normalized L_2 norm used to study the convergence of the method is:

$$Normalized\ \ L_2\ \ norm = \frac{\sqrt{\int_\Omega \psi^2 d\Omega}}{Number\ of\ nodes} \tag{4.16}$$

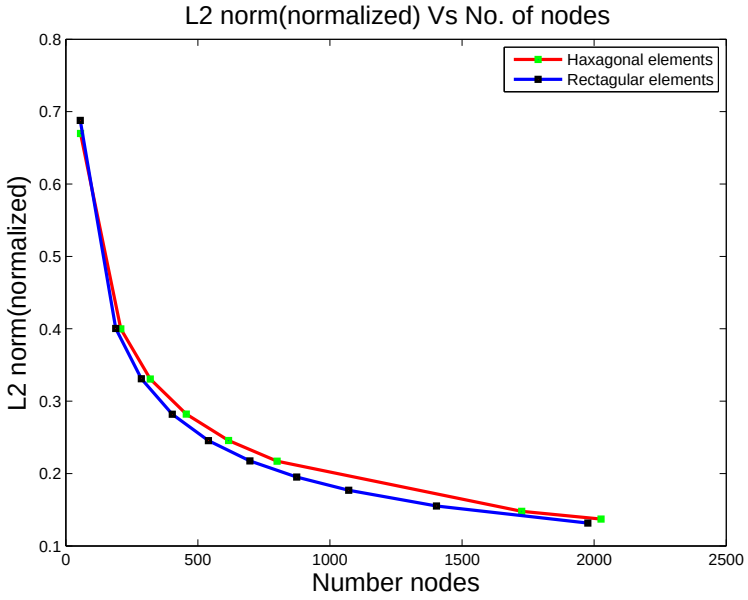

Figure 4.7: Convergence of normalized L_2 norm given in Eq. (4.16) for both rectangular elements and hexagonal elements.

In this chapter the new integration technique based on Schwarz-Christoffel conformal mapping have been applied on the few bench mark problems like static and free vibration analysis of a cantilever beam. The overall convergence of the method for both static and dynamic case was studied and proved that the new integration technique works good

to obtain stiffness and mass matrix and to solve static analysis and structural vibration problems. Therefore, the method can be effectively used to analyze the polycrystalline material, where each polycrystalline material can be taken as a polygonal element. Moreover, the method can be effectively used for complex geometries.As positivity of the jacobian is always guaranteed irrespective of convexity of the polygon the method yields good results even for distorted elements. In this method elements used were hexagonal shape which are distorted elements when compared to the quadrilateral elements. Thus the method can be effectively used even with the distorted elements which is not possible in the standard FEM. In the next chapter the same integration technique is extended and applied for linear elastic fracture mechanics problem and convergence of the method is examined for the mode-I crack problem.

Chapter 5

Polygonal XFEM based on Schwarz-Christoffel Conformal Mapping

Solving Linear Elastic Fracture Mechanics (LEFM) problem using standard finite element method requires fine mesh and geometry of the mesh should conform with the crack geometry in the domain. For each crack a separate refinement to the mesh is required to solve the LEFM problem with remeshing for a new crack dimension. Mesh refinement and meshing can be avoided by using Extended Finite Element Method (XFEM) proposed by Belytschko and Dolbow [33], in which a back ground mesh without crack can be used to solve the LEFM problem. In XFEM using Gauss quadrature method, elements can not have more than four edges and convexity of the elements need to be ensured to have positive jacobian. In this chapter an XFEM using polygonal finite element method is proposed and integration over the polygon is carried by Schwarz Christoffel mapping [15] given in [11]. The overall approach is validated using a successful convergence study of a mode-I crack in a thick beam bending problem.

5.1 Extended Finite Element Method (XFEM)

Modeling of fracture and failure remains one of the most challenging problems in mechanics. Finite element analysis using singular elements as well as enriched elements are reasonably effective in the analysis of stationery cracks. To model a crack using these methods, meshing should conform to the crack geometry and complexity further increases if the crack is irregular. To avoid these difficulties an extended Finite Element Method (XFEM) has been proposed by Belytschko and Dolbow [33]. In this method crack is modeled using a background mesh and elements in which crack exists are enriched. Elements used are of triangular or quadrilateral shapes. For domains having complex geometry very fine mesh is required near the stress concentration regions. Moreover, convexity of the element should be maintained to avoid negative jacobian. As a consequence cost of computation is high for such complex geometry. Polygonal finite elements are a generalization of triangular and quadrilateral finite element methods to meshes with n-sided elements ($n \geq 3$). Polygonal finite elements provide greater flexibility in meshing. Integration over a polygonal element can be done using Polygonal finite element method proposed by Sundararajan *et al.* [11] in which a polygon is mapped to unit disk and integration is carried over the unit disk.

5.2 Governing equations and weak form

The governing equilibrium equations for a 2D static elasticity problem defined in the domain Ω bounded by Γ and $\Gamma = \Gamma_u \cup \Gamma_t$, $\Gamma_u \cap \Gamma_t = \phi$ can be expressed as

$$\nabla_s^{\mathrm{T}} \boldsymbol{\sigma} + \mathbf{b} = \mathbf{0} \quad \text{in } \Omega \tag{5.1}$$

Where $\mathbf{0}$ is a null vector, $\boldsymbol{\sigma}$ is the stress tensor and $\mathbf{b}$ is the vector of external forces. The following are the prescribed boundary conditions

$$\mathbf{u} = \overline{\mathbf{u}} \ \textit{in} \ \Gamma_u \tag{5.2}$$

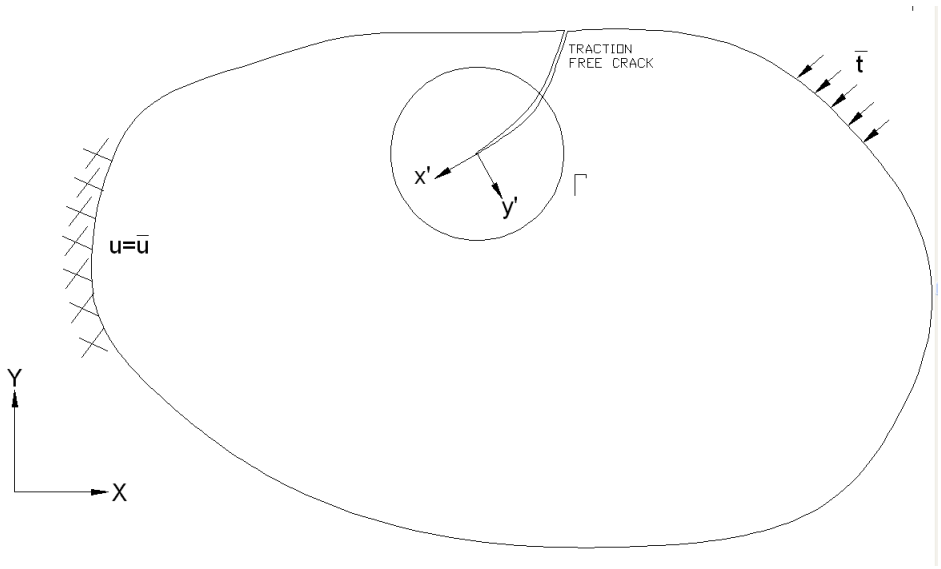

Figure 5.1: A Schematic diagram showing a stable crack in a two-dimensional body under global equilibrium.

$$\mathbf{n}^T\boldsymbol{\sigma} = \bar{\mathbf{t}} \ \ on \ \ \Gamma_t \tag{5.3}$$

$$\mathbf{n}^T\boldsymbol{\sigma} = \mathbf{0} \ \ on \ \ \Gamma_c \tag{5.4}$$

where $\overline{\mathbf{u}} = (\overline{u}_x, \overline{u}_y)^T$ is the prescribed displacement vector on the essential boundary Γ_u; $\mathbf{t} = (\bar{t}_x, \bar{t}_y)^T$ is the prescribed traction vector on the natural boundary Γ_t and Γ_c is the traction boundary; $\mathbf{n}$ is the unit outward normal vector. The discrete version of the weak form for this problem are obtained using Galerkin approach as

$$\int_\Omega (\bigtriangledown_s \delta\mathbf{u})^T \mathbb{D} (\bigtriangledown_s \delta\mathbf{u}) d\Omega - \int_\Gamma (\delta\mathbf{u}^T)\mathbf{b} d\Omega - \int_\Gamma (\delta\mathbf{u})^T \bar{\mathbf{t}} d\Gamma = 0 \tag{5.5}$$

where $\mathbf{u}$ and $\delta\mathbf{u}$ are the test functions that belong to Sobolev space of functions and $\mathbb{D}$ is the constitutive matrix. The Finite element method uses the following trial and test functions:

$$\mathbf{u}^h(\mathbf{x}) = \sum_{i=1}^{NP} \mathbf{N}_i(\mathbf{X})\mathbf{d}_i + \sum_{j=1}^{m} \mathbf{N}_k(\mathbf{X})\psi(\mathbf{X})\mathbf{a}_k \tag{5.6a}$$

$$\delta\mathbf{u}^h(\mathbf{x}) = \sum_{i=1}^{NP} \mathbf{N}_i(\mathbf{X})\delta\mathbf{d}_i + \sum_{j=1}^{m} \mathbf{N}_k(\mathbf{X})\psi(\mathbf{X})\delta\mathbf{a}_k + \sum_{j=1}^{m} \mathbf{N}_k(\mathbf{X})\delta\psi(\mathbf{X})\mathbf{a}_k \tag{5.6b}$$

where NP is the total number of nodes in the mesh, k is the number of enriched nodes, $\mathbf{a}_k$ is the set of degrees of freedom added to the standard finite element modal degrees of freedom and $\psi(\mathbf{X})$ is the discontinuous enrichment function.

$$\mathbf{N}_i = \begin{bmatrix} N_i & 0 \\ 0 & N_i \end{bmatrix} \tag{5.7}$$

represents the shape functions matrix of degree p associated with node i, $\mathbf{d}_i = [u_i, v_i]^T$ are the degrees of freedom associated with node i. By substituting the approximations $\mathbf{u}^h$ and $\delta\mathbf{u}^h$ into the weak form and invoking the arbitrariness of virtual nodal displacements, Equation (5.5) yields the standard discretized algebraic system of equations:

$$\mathbf{Kd} = \mathbf{f} \tag{5.8}$$

with the stiffness matrix given by

$$\mathbf{K_{ij}^e} = \begin{bmatrix} \mathbf{K}_{ij}^{\mathbf{uu}} & \mathbf{K}_{ij}^{\mathbf{ua}} & \mathbf{K}_{ij}^{\mathbf{uc}} \\ \mathbf{K}_{ij}^{\mathbf{au}} & \mathbf{K}_{ij}^{\mathbf{aa}} & \mathbf{K}_{ij}^{\mathbf{ac}} \\ \mathbf{K}_{ij}^{\mathbf{cu}} & \mathbf{K}_{ij}^{\mathbf{ca}} & \mathbf{K}_{ij}^{\mathbf{cc}} \end{bmatrix} \tag{5.9}$$

and the load vector by

$$\mathbf{f_i} = \begin{bmatrix} \mathbf{f_i^u} & \mathbf{f_i^a} & \mathbf{f_i^{c1}} & \mathbf{f_i^{c2}} & \mathbf{f_i^{c3}} & \mathbf{f_i^{c4}} \end{bmatrix}^T \tag{5.10}$$

$\mathbf{d}$ is a vector of nodal parameters:

$$\mathbf{d^h} = \begin{bmatrix} \mathbf{d} & \mathbf{a} & \mathbf{c1} & \mathbf{c2} & \mathbf{c3} & \mathbf{c4} \end{bmatrix}^T \tag{5.11}$$

with

$$\mathbf{K_{ij}^{rs}} = \int_{\Omega^h} (\mathbf{B_i^r})^{\mathbf{T}} \mathbf{D} (\mathbf{B_j^s}) d\Omega \quad (r, s = \mathbf{d}, \mathbf{a}, \mathbf{c}) \tag{5.12}$$

$$\mathbf{f_i^u} = \int_{\Omega^h} N_i \mathbf{b} d\Omega + \int_{\Gamma_t} N_i \bar{t} d\Gamma \tag{5.13}$$

$$\mathbf{f_i^a} = \int_{\Omega^h} N_i H \mathbf{b} d\Omega + \int_{\Gamma_t} N_i H \bar{t} d\Gamma \tag{5.14}$$

$$\mathbf{f_i^{b\alpha}} = \int_{\Omega^h} N_i F_\alpha \mathbf{b} d\Omega + \int_{\Gamma_t} N_i F_\alpha \bar{t} d\Gamma \tag{5.15}$$

where Ω_h is the discretized domain, formed by the union of elements Ω_e. The stiffness matrix $\mathbf{K}$ is symmetric, positive definite and with a strain-displacement matrix defined as

$$\mathbf{B_i^u}(\mathbf{x}) = \bigtriangledown_s N_i(\mathbf{x}) = \begin{bmatrix} \frac{\partial N_i}{\partial x} & 0 \\ 0 & \frac{\partial N_i}{\partial y} \\ \frac{\partial N_i}{\partial y} & \frac{\partial N_i}{\partial x} \end{bmatrix} \tag{5.16}$$

$$\mathbf{B_i^a}(\mathbf{x}) = \begin{bmatrix} \frac{\partial (N_i H)}{\partial x} & 0 \\ 0 & \frac{\partial (N_i H)}{\partial y} \\ \frac{\partial (N_i H)}{\partial y} & \frac{\partial (N_i H)}{\partial x} \end{bmatrix} \tag{5.17}$$

$$\mathbf{B_i^b} = \begin{bmatrix} \mathbf{B_i^{c1}} & \mathbf{B_i^{c2}} & \mathbf{B_i^{c3}} & \mathbf{B_i^{c4}} \end{bmatrix} \tag{5.18}$$

$$\mathbf{B_i^\alpha}(\mathbf{x}) = \begin{bmatrix} \frac{\partial (N_i F_\alpha)}{\partial x} & 0 \\ 0 & \frac{\partial (N_i F_\alpha)}{\partial y} \\ \frac{\partial (N_i F_\alpha)}{\partial y} & \frac{\partial (N_i F_\alpha)}{\partial x} \end{bmatrix} \tag{5.19}$$

where, i in equation (5.16) is an arbitrary node of the element. The size of the $\mathbf{B}$ matrix depends on the number of nodes in an element. To include the effect of interpolants, the following shifting amendments are required.

$$\mathbf{B_i^a}(\mathbf{x}) = \begin{bmatrix} \frac{\partial (N_i[H(\xi) - H(\xi_i)])}{\partial x} & 0 \\ 0 & \frac{\partial (N_i[H(\xi) - H(\xi_i)])}{\partial y} \\ \frac{\partial (N_i[H(\xi) - H(\xi_i)])}{\partial y} & \frac{\partial (N_i[H(\xi) - H(\xi_i)])}{\partial x} \end{bmatrix} \tag{5.20}$$

$$\mathbf{B_i^\alpha}(\mathbf{x}) = \begin{bmatrix} \frac{\partial (N_i(F_\alpha - F_{\alpha i}))}{\partial x} & 0 \\ 0 & \frac{\partial (N_i(F_\alpha - F_{\alpha i}))}{\partial y} \\ \frac{\partial (N_i(F_\alpha - F_{\alpha i}))}{\partial y} & \frac{\partial (N_i(F_\alpha - F_{\alpha i}))}{\partial x} \end{bmatrix} \tag{5.21}$$

where $\alpha = 1, 2, 3$ and 4 in equation (5.21) and (5.19).

5.2.1 Enrichment functions

The following crack face and crack tip enrichment were used in the present work.

1. $\psi(\mathbf{x}) = H(\xi)$ with $H(\xi)$ heaviside function. Derivative of the heaviside function is the Dirac delta function, which vanishes except at the position of the crack interface, that is $H_{,}(\xi) = \delta(\xi)$,

$$H_{,i}(\xi) = \begin{cases} 1 & : \quad \text{at crack} \\ 0 & : \quad \text{otherwise} \end{cases}$$

As a result equation (5.17) can be rewritten as

$$\mathbf{B}_i^{\mathbf{a}}(\mathbf{x}) = \begin{bmatrix} \frac{\partial(N_i)}{\partial x}H & 0 \\ 0 & \frac{\partial(N_i)}{\partial y}H \\ \frac{\partial(N_i)}{\partial y}H & \frac{\partial(N_i)}{\partial x}H \end{bmatrix} \tag{5.22}$$

2. The near tip enrichment function is given as $\psi = F_\alpha(r,\theta)$. The near tip enrichment functions are defined in terms of local coordinates (r,θ), that is,

$$F_\alpha(r,\theta) = \left\{ \sqrt{r}\sin\tfrac{\theta}{2}, \quad \sqrt{r}\cos\tfrac{\theta}{2}, \quad \sqrt{r}\sin\theta\sin\tfrac{\theta}{2}, \quad \sqrt{r}\sin\theta\cos\tfrac{\theta}{2} \right\} \tag{5.23}$$

Derivatives of F_α with respect to the crack tip polar coordinates (r,θ) become

$$\begin{aligned} F_{1,r} &= \tfrac{1}{2\sqrt{r}}\sin\tfrac{\theta}{2}, & F_{1,\theta} &= \tfrac{\sqrt{r}}{2}\cos\tfrac{\theta}{2} \\ F_{2,r} &= \tfrac{1}{2\sqrt{r}}\cos\tfrac{\theta}{2}, & F_{2,\theta} &= \tfrac{\sqrt{r}}{2}\sin\tfrac{\theta}{2} \\ F_{3,r} &= \tfrac{1}{2\sqrt{r}}\sin\tfrac{\theta}{2}\sin\theta, & F_{3,\theta} &= \sqrt{r}(\tfrac{1}{2}\cos\tfrac{\theta}{2}\sin\theta + \sin\tfrac{\theta}{2}\cos\theta) \\ F_{4,r} &= \tfrac{1}{2\sqrt{r}}\cos\tfrac{\theta}{2}\sin\theta, & F_{4,\theta} &= \sqrt{r}(-\tfrac{1}{2}\sin\tfrac{\theta}{2}\sin\theta + \cos\tfrac{\theta}{2}\cos\theta) \end{aligned} \tag{5.24}$$

The derivatives of $F_\alpha(r,\theta)$ with respect to the local coordinate system (x',y') are

defined as

$$\begin{aligned} F_{1,x'} &= -\tfrac{1}{2\sqrt{r}}\sin\tfrac{\theta}{2}, & F_{1,y'} &= \tfrac{1}{2\sqrt{r}}\cos\tfrac{\theta}{2} \\ F_{2,x'} &= \tfrac{1}{2\sqrt{r}}\cos\tfrac{\theta}{2}, & F_{2,y'} &= \tfrac{1}{2\sqrt{r}}\sin\tfrac{\theta}{2} \\ F_{3,x'} &= -\tfrac{1}{2\sqrt{r}}\sin\tfrac{3\theta}{2}\sin\theta, & F_{3,y'} &= -\tfrac{1}{2\sqrt{r}}(\sin\tfrac{\theta}{2}+\sin\tfrac{3\theta}{2}\cos\theta) \\ F_{4,x'} &= -\tfrac{1}{2\sqrt{r}}\cos\tfrac{3\theta}{2}\sin\theta, & F_{4,y'} &= \tfrac{1}{2\sqrt{r}}(\cos\tfrac{\theta}{2}+\cos\tfrac{3\theta}{2}\cos\theta) \end{aligned} \tag{5.25}$$

Finally, the derivatives of $F_\alpha(r,\theta)$ in the global coordinate system is obtained as

$$F_{\alpha,x} = F_{\alpha,x'}\cos(\beta) + F_{\alpha,y'}\sin(\beta) \tag{5.26a}$$

$$F_{\alpha,y} = -F_{\alpha,x'}\sin(\beta) + F_{\alpha,y'}\cos(\beta) \tag{5.26b}$$

Where β is the angle of crack path with respect to x-axis.

5.3 Stress Intensity Factor (SIF)

The stress intensity factor is the one of the important parameters representing the properties of crack tip. In this work the domain integral method proposed by Kim and Paulino [35] is used to compute stress intensity factors. The path independent J integral for the cracked body is defined as [34]

$$J = \int_\Gamma \left(W_s\delta_{1j} - \sigma_{ij}\frac{\partial u_j}{\partial x'} \right) \mathbf{n_j} d\Gamma \tag{5.27}$$

Where $\mathbf{n_j}$ is the jth component of the outward unit normal to Γ, δ_{1j} is Kronecker delta, W_s is the strain energy density for linear elastic material, and Γ is an arbitrary contour around the crack tip which encloses no other cracks and discontinuities. The Equation (5.27) is not suited for the finite element implementation , and therefore an equivalent form of J integral can be obtained by exploiting the divergence theorem in the form of

domain integral approach given by Kim and Paulino [36]

$$J = -\int_A \left(W_s \delta_{1j} - \sigma_{ij} \frac{\partial u_i}{\partial x'} \right) \frac{\partial q}{\partial x_j} d\Gamma \tag{5.28}$$

where A is the area surrounding the crack tip and q is the smoothly varying function. Γ can be assumed as circle or rectangle whose center is at crack tip. In the present work Γ is taken as a circle. As proposed by Dolbow and Moes*et al* [37], a simple function q, varying linearly from q =1 at the crack tip to q = 0 at the exterior boundary Γ as shown in figure 5.2, is used in the finite element model. Therefore, the elements away from the boundary can be neglected. It is worth noting that the value within the parentheses in Eq. (5.28) is not necessary to be evaluated in the area that q is constant (and so its gradient vanishes). From a numerical aspect, in spite of the fact that the stress gradient in elements containing a crack tip is usually very high, it is more appropriate to avoid locating the contour on the elements including a crack tip. The method of interaction integral, based on the definition of an auxiliary state, is used to extract mixed mode stress intensity factors. Suppose there are two equilibrium states; state 1 corresponds to the actual state and state 2 corresponds to an auxiliary state for the given problem geometry. Auxiliary stress and strain states should be chosen so as to satisfy both the equilibrium equation and the traction free boundary condition on the crack surface in the area A. J-integral domain is shown in figure 5.2.

5.4 Numerical integration of weak form for Poly-XFEM

The Finite Element stiffness matrix given in equation (5.9) must be evaluated over the element. In conventional finite element method an element does not have more than four edges for 2D domains. In general, the Gau$\mathcal{B}$ quadrature rule can be effectively used to integrate the weak forms. To integrate weak forms over the *n-gon* no general quadrature rule is available. Again, for this poly-XFEM the new integration scheme

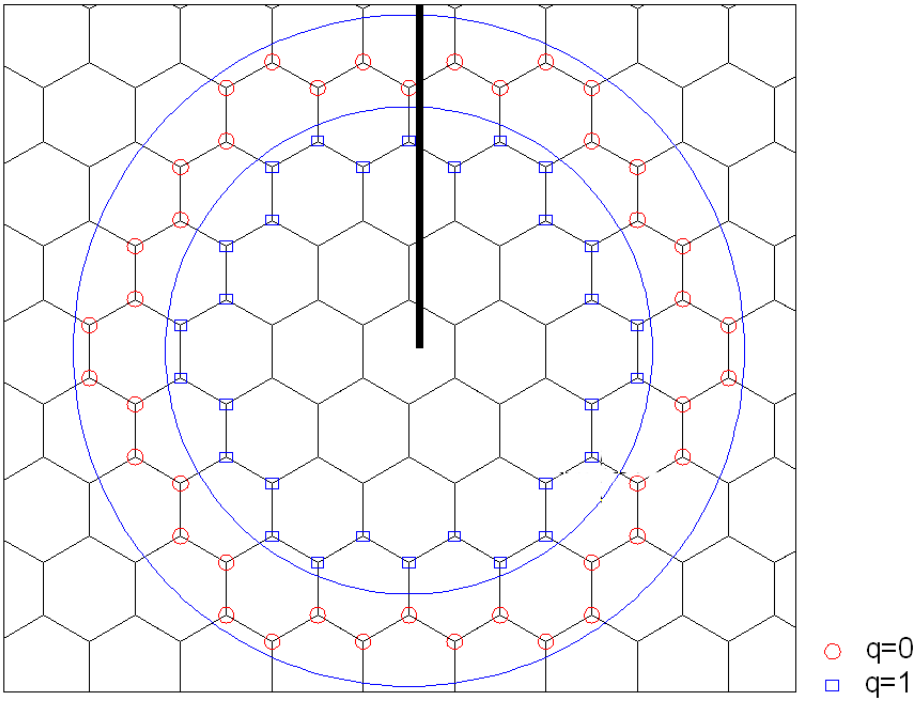

Figure 5.2: J-integral domain for polygonal elements with crack. Nodal values for function q.

based on SC mapping proposed by sundararajan *et al* [11] is used to integrate the weak form. Moreover, subdivision of elements which are divided by crack is not required in the new integration scheme, which is otherwise required in XFEM based on standard Finite Element Method.

5.5 Edge Crack With Mode-I Loading

In this paper the Poly-XFEM-SCCM has been applied to mode-I problem and convergence of Mode-I Stress Intensity Factor for an edge crack has been established. For this problem a polygonal mesh has been developed as shown in figure 5.4. A 2D bar of dimensions L=10, D=3 and B=1 having mechanical properties E=3e7, $\nu = 0.3$, was considered for the edge crack problem. The geometry and loading and boundary conditions are shown in figure 5.3 with $\sigma = 100$. Analytical value of the stress intensity factor

for the edge crack is given by

$$K_I = F(a/D)\sigma\sqrt{\pi a} \tag{5.29}$$

and we shall use this analytical solution result as reference for convergence study. Where a is the crack length, D is the plate width and $F(a/b)$ is an empirical function given (For $(a/d) \leq 0.6$)

$$F(a/b) = 1.12 - 0.231(a/D)10.55(a/D)^2 - 21.72(a/D)^3 + 30.39(a/D)^4 \tag{5.30}$$

Normalized stress intensity factor (SIF) is given as

$$Normalized\ stress\ intensity\ factor = K_I/\sigma. \tag{5.31}$$

Here σ is the far field stress. Convergence of the normalized mode-I SIF given in Eq. (5.31) with increasing number of polygonal elements (hexagons in this example) is shown in figure 5.6 and relative error in SIF is shown in figure 5.7. Error decreases as number of polygonal elements are increased. From this convergence study it is observed that the new integration scheme given in [11] yields good results for LEFM problem using polygonal elements.

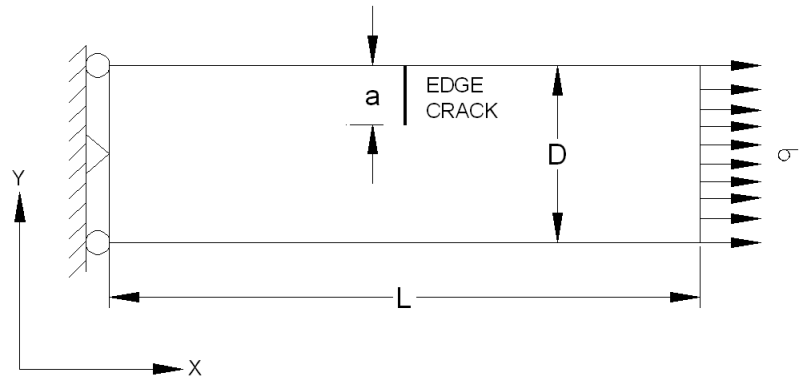

Figure 5.3: A 2D domain with edge crack subjected to axial loading σ at one of the edge.

In this work, the new integration scheme [11] for arbitrary polygons was used to

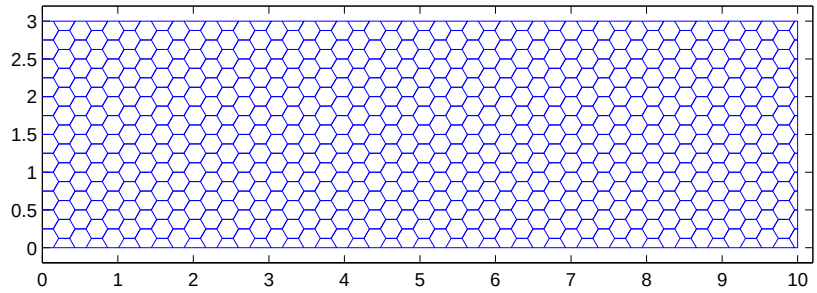

Figure 5.4: Polygonal background mesh used for 2D edge crack problem.

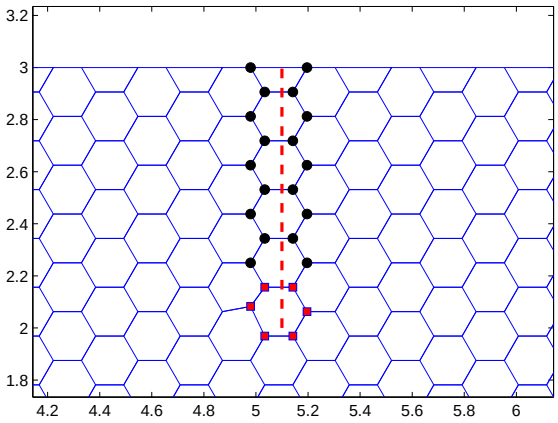

Figure 5.5: Enriched nodes indicated with square marks are the nodes surrounding the crack tip. Nodes indicated with circle heaviside enriched. These nodes are involved in the additional degrees of free dom due to XFEM.

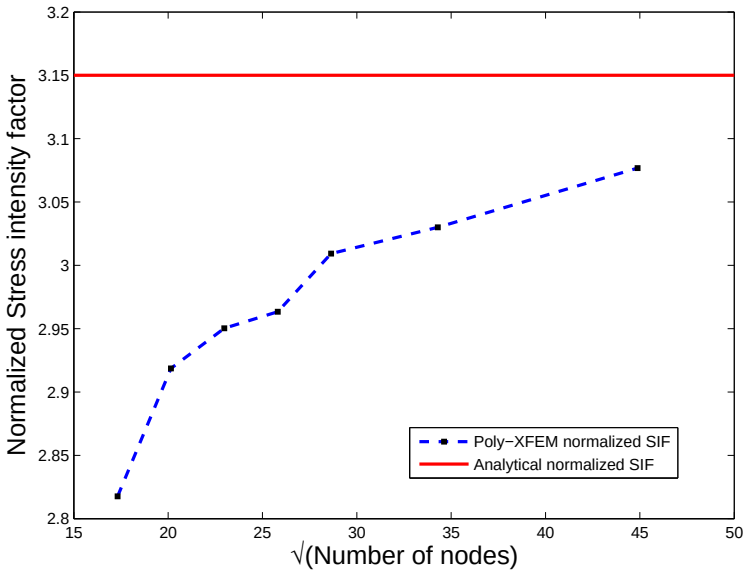

Figure 5.6: Convergence of normalized SIF given Eq. (5.31) for K-I with number of elements for the edge crack problem.

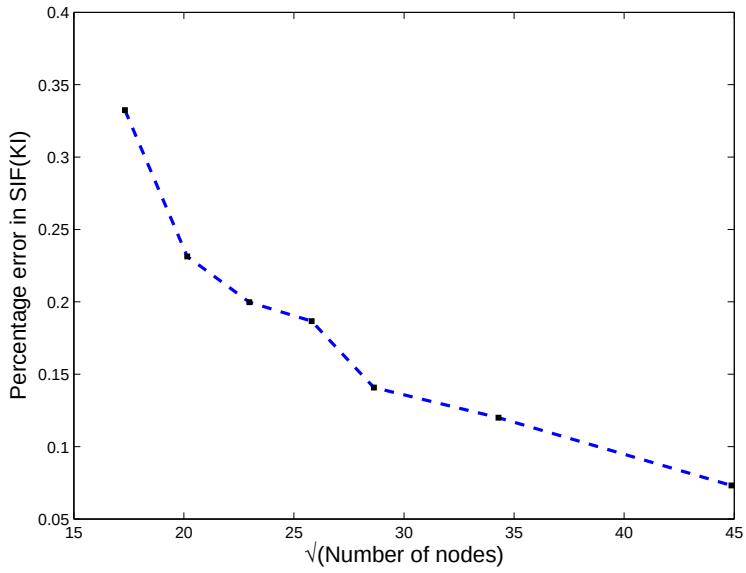

Figure 5.7: The convergence of percentage error in SIF for K-I with number of nodes.

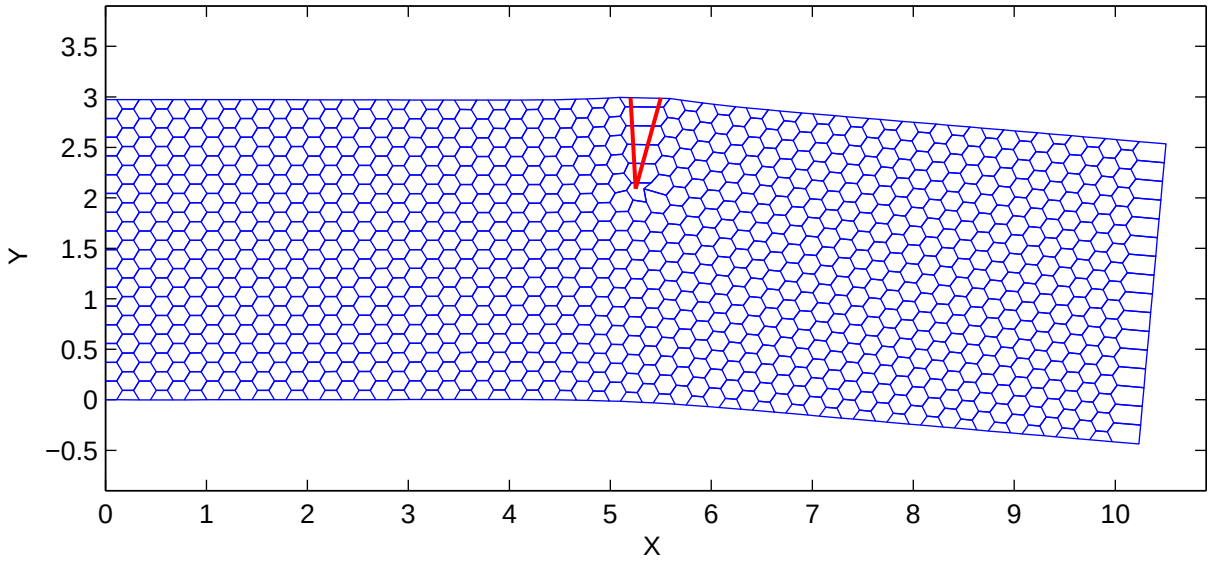

Figure 5.8: Deformed shape of the bar with edge crack subjected to far filed stress σ (Deformation magnification factor = 30).

integrate singular, discontinuous functions in stiffness matrix and J integral to compute stress intensity factor. It has been shown that the method converges with mesh refinement. Moreover, further subdivision of elements can be avoided in this new integration approach. As elements used are polygon, the method can be effectively used to analyse the polycrystal structural behavior. Moreover, positivity of jacobian is always guaranteed whether the element is convex or concave, the method can be effectively used for a mesh having distorted elements.

Chapter 6

Conclusions and Future Work

6.1 Summary on the completed work

In the context of two-dimensional elasto-static and free vibration problem using polygonal finite element method based on Schwarz-Christoffel conformal mapping was presented. And in the context of linear elastic fracture mechanics, the enriched polygonal finite element method, called polygonal eXtended Finite Element Method (poly-sccm-XFEM), was presented using the same integration method. The method has been successfully applied to static, free vibration and LEFM problem and convergence of the method was shown. It has been proved that there is no need for further subdivision of elements having crack in the new integration scheme.

In this work polygonal element in physical domain is mapped to unit disk using Schwarz-Christoffel conformal mapping. Since positivity of jacobian is always guaranteed irrespective of the element convexity, the method can be effectively used to distorted elements. A **FORTRAN** code using SCPACK subroutines together with non-linear equation solver, banded solver and banded eigen value solver etc., was developed to solve polygonal Finite Element Method based on Schwarz-Christoffel conformal mapping for static, free vibration (eigen value problem) and LEFM problem.

The main advantages of the method are: (1) only one level of mapping is required, (2) positivity of jacobian is always guaranteed, and (3) subdivision of elements which

are having crack is not required for integration.

6.2 Application and Future Work

This thesis work could be considered as a initial step in the way to learn and apply the polygonal finite element and poly XFEM to real applications. The method has been developed here in two dimensions, and a more challenging project would be to extend to three dimensions. Polycrystalline materials have crystal structures in the form of polygonal shapes. To analyse the polycrystal structure using standard Finite Element Method, each crystal is again subdivided into finite elements. Using Poly-SCCM method, each element can be taken as polygonal element. Interface and grain boundary effects are to be considered in the formulation. Since Poly-SCCM can also be applied to LEFM problems by using enrichment functions, polycrystalline material with crack can be modeled. The method can be extended to find the natural frequency of a structure having strong or weak discontinuity.

Bibliography

[1] R. Courant, Variational Methods for the solution of problems of equilibrium and vibrations, *Bulletin of the American Mathematical Society*, Vol.49, 1943, 1-23.

[2] Zienkiewicz. O.C., Talor, R.L. and Zhu, J.H. *The Finite Element Method,* 6th edn. Elssevier, USA.

[3] T.P. Fries and H.G. Matthies. Classification and over view of mesh free methods. Informatirkbericht Report 2003-03, Institute of scientific domputing, Technical University Braunschweig, Hans-Sommer-Strasse 65, D38106 Braunschweig, March 2003.

[4] Canuto C., Hussaini M. Y., Quarteroni A., and Zang T.A. (2006) Spectral Methods. Fundamentals in Single Domains. Springer-Verlag, Berlin Heidelberg

[5] P. Solin, K. Segeth, I. Dolezel: Higher-Order Finite Element Methods, Chapman and Hall/CRC Press, 2003

[6] I. Babuska, B.Q. Guo: The h, p and h-p version of the finite element method: basis theory and applications, *Advances in Engineering Software*, Volume 15, Issue 3-4, 1992.

[7] Babuska, Ivo; Uday Banerjee, John E. Osborn (June 2004). "Generalized Finite Element Methods: Main Ideas, Results, and Perspective". *International Journal of Computational Methods* 1 : 67103. doi:10.1142/S0219876204000083

[8] S. Brenner, R. L. Scott, The Mathematical Theory of Finite Element Methods, 2nd edition, Springer, 2005

[9] G.R. Liu, K.Y. Dai, and T.T. Nguyen. A smoothed Finite element for mechanics problems. *Computational Mechanics*, DOI 10.1007/s00466-006-0075-4, 2006.

[10] N. Sukumar and A. Tabarraei. Conforming polygonal finite elements.*International Journal for Numerical Methods in Engineering*, 61(2045-2066), 2004.

[11] Natarajan. S, Boardas SP, Mahapatra DR. Numerical integration over arbitrary polygonal domains based on Schwarez-Christoffel conformal mapping.*International Journal of numerical methods in Engineering.* 2009; doi:10.1002/nme.2589.

[12] Suvranu De and Klaus-Jurgen Bathe. The method of finite spheres with improved numerical integration. *Computers and structures*, 79(1), 2001.

[13] N. Moaes, J. Dolbow, and T. Belytschko. A Finite element method for crack growth without remeshing. *International Journal for Numerical Methods in Engineering*, 46(1):131-150,1999.

[14] L. N. Trefethen. Numerical conformal mapping. *SIAM J Sci Stat Comput*, 1(1):82-102, 1980.

[15] A Tobin Driscoll and N Lloyd Trefethen. Schwarz christoffel mapping. *Cambridge Monographs on Applied and Computational Mathematics*, 8(1), 2002.

[16] H. Nguyen-Xuan, Stephane Bordas, and H. Nguyen-Dang. A smoothed finite element method for shells. *Computer Methods in Applied Mechanics and Engineering*, accepted,2008.

[17] W H Peirce. Numerical integration over the planar annulus. *J soc Ind Appl Math, 5(2):66-73, 1957.*

[18] J.W. Yoo, B. Moran, and J.S. Chen. Stabilized conforming nodal integration in the natural-element method. *International Journal for Numerical Methods in Engineering*, 60:861-890, 2004.

[19] Suvranu De and Klaus-Jurgen Bathe. The method of finite spheres with improved numerical integration. *Computers and structures*, 79(1), 2001.

[20] E. L. Wachspress. A rational basis for function approximation. Lecture notes in Mathematics, 1971.

[21] N. Sukumar and E.A. Malsch. Recent advances in the construction of polygonal finite element interpolants. *Archives of Computational Methods in Engineering*, 13(1):129-163, 2006.

[22] Gautham Dasgupta. Interpolants within convex polygons: Wachspress' shape functions.*ASCE - Journal of aerospace engineering*, 16(1-8), 2003.

[23] N. Sukumar. The Natural Element Method in Solid Mechanics. PhD thesis, Theoretical and Applied Mechanics, Northwestern University, Evanston, IL, U.S.A, 1998.

[24] N. Sukumar. Construction of polygonal interpolants: A maximum entropy approach. *International Journal for Numerical Methods in Engineering*, 61(12):2159-2181, 2004.

[25] E. Cueto, N. Sukumar, B. Calvo, M.A. Martinez, J. Cegonino, and M. Doblare. Overview and recent advances in natural neighbour galerkin methods. *Archives of Computational Methods in Engineering*, 10(4):307-384, 2003.

[26] N. Sukumar, B. Moran, and T. Belytschko. The natural element method in solid mechanics. International Journal for Numerical Methods in Engineering, 43(5):839-887, 1998.

[27] M. Meyer, H. Lee, and A. H. Barr. Generalized barycentric coordinates for irregular n-gons. *Journal of Graphics Tools*, 7(1):13-22, 2002.

[28] J. Warren, S. Schaefer, A. Hirani, and M. Desbrun. Barycentric coordinates for convex sets. *Advances in Computational Mechanics*,27(3):319-338, 2007.

[29] J. Warren. On the uniqueness of barycentric coordinates. *Contemporary Mathematics*, Proceedings of AGGM02, pages 93-99, 2003.

[30] M. Meyer H. Lee and A. H. Barr. Generalized barycentric coordinates for irregular n-gons. *Journal of Graphics Tools*, 7(1):13-22, 2002.

[31] N Sukumar, B Moran, and T Belytschko. The natural element method in solid mechanics. *International Journal for Numerical Methods in Engineering*, 43:839-887, 1998.

[32] S. P. Timoshenko and J. N. Goodier. Theory of elasticity. Mc-Graw-Hill, New York, 1970.

[33] N. Moaes, J. Dolbow, and T. Belytschko. A Finite element method for crack growth without remeshing. *International Journal for Numerical Methods in Engineering*, 46(1):131-150,1999.

[34] Rice,J.R. Path independent integral and the approximationanalysis of strain concentration by notches and cracks. *Journal of Applied mechanics*,**55**,98-103.

[35] Kim, J.H. and Paulino. Mixed mode fracture of orthotropic functionally graded materialas using finte elemets and the modified crack closure method. *Engineering Fracture mechanics*,**69**,1557-1586.

[36] Kim, J.H. and Paulino. The interaction integral for fracture of orthotropic functionally graded materials using finite elements and the modified crack closure method. *International Journal of solids and structures*,**40**,3967-4001.

[37] Moes, N., Dolbow, J. and Belytschko, T. A finite element method for crack growth without remeshing. *International Journal for Numerical Methods in Engineering*, 46, 131150.

[38] N. Hu, H. H. Wang, B. Yan, H. Fukunaga, D. Roy Mahapatra, S. Gopalakrishnan. The partition of unity finite element method for elastic wave propagation in

ReissnerMindlin plates. *International journal for numerical methods in engineering*, 2007; **70**: 14511479.